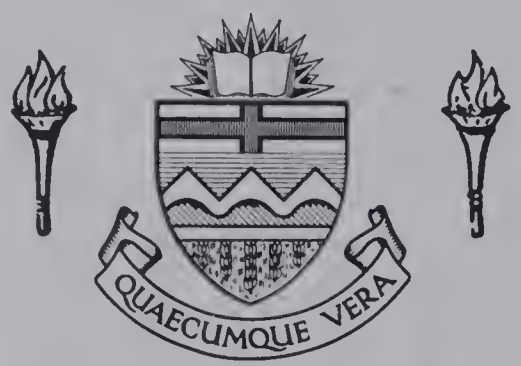

The University of Alberta
Printing Department
Edmonton, Alberta

THE UNIVERSITY OF ALBERTA

RADIATIVE LIFETIME MEASUREMENTS FOR OXYGEN AND NITROGEN IONS

by

© CHII-CHAN LIN

A THESIS

SUBMITTED TO THE FACULTY OF GRADUATE STUDIES

IN PARTIAL FULFILMENT OF THE REQUIREMENTS FOR THE DEGREE

OF MASTER OF SCIENCE

DEPARTMENT OF PHYSICS

EDMONTON, ALBERTA

SEPTEMBER, 1968

UNIVERSITY OF ALBERTA

FACULTY OF GRADUATE STUDIES

The undersigned certify that they have read, and recommend to the Faculty of Graduate Studies for acceptance, a thesis entitled RADIATIVE LIFETIME MEASUREMENTS FOR OXYGEN AND NITROGEN IONS, submitted by Chii-Chan Lin in partial fulfilment of the requirements for the degree of Master of Science.

ABSTRACT

The beam-foil technique has been applied to make photoelectric measurements of radiative lifetimes for energy levels in ionized oxygen and nitrogen atoms. The wavelength range covered was 1800-5500 Å. Lifetimes have been obtained for 14 transitions involving nitrogen, 10 involving oxygen and 11 unassigned transitions, from decay curves following a single exponential. A computer analysis has also been tried in 42 cases for which the curves followed a non-exponential decay due to cascade repopulation of the radiating level. These results are compared with those obtained by other workers and with theoretical calculation where it is available. Finally an independent measurement of the beam velocity is described, which indicates an energy loss for O_2^+ ions at 1 MeV incident on a 10 $\mu g/cm^2$ carbon foil of around 8%, in agreement with that to be expected theoretically.

ACKNOWLEDGEMENTS

I would like to thank my supervisor, Dr. E. H. Pinnington, for initiating and participating in the project and for his encouragement and guidance throughout the past two years.

I would also like to express my gratitude to Dr. G. R. Freeman of the Radiation Research Committee for the use of the Van de Graaff accelerator. Special thanks are due to Mr. E. B. Cairns for his technical assistance in the operation of the accelerator.

To Mr. N. Riebeek, I am grateful for assistance in the design and construction of the target chambers.

Finally, I wish to thank the University of Alberta and the National Research Council for financial support.

TABLE OF CONTENTS

TABLE OF CONTENTS (Continued)

LIST OF ILLUSTRATIONS

LIST OF TABLES

CHAPTER I

INTRODUCTION

1.1 Necessity for Radiative Lifetime Measurements for Ionized Atoms

In the spectroscopic determination of the composition of plasmas, laboratory or celestial, it is necessary to know the atomic parameter which governs the intensity of the spectrum line. This parameter is known as the oscillator strength or f-value and is the number of classical oscillators per atom which would absorb the same amount of radiation from a parallel beam of light. The f-value is determined ultimately by the quantum mechanical wavefunctions of the two states involved in the transition. Thus for a transition from a state i to a state j, the f-value for the transition, f_{ij}, is given by (Di 52)

$$f_{ij} = \frac{8\pi^2}{3h} m\nu_{ij} \vec{r}_{ij} \vec{r}^{*}_{ij} \qquad (1.1)$$

where $\vec{r}_{ij} = \int \Psi_i \vec{r} \Psi_j^{*} d\tau$

and $\vec{M}_{ij} = 2e\vec{r}_{ij}\cos(2\pi\nu_{ij}t)$ is the moment of the electric dipole oscillator of frequency ν_{ij}. The intensity of the spectrum line is then given by

$$I = \int I_\nu d\nu = \frac{1}{4\pi} N_i A_{ij} l h\nu_{ij} \qquad (1.2)$$

where N_i = number density of atoms in state i,

l = thickness of emitting layer (provided that the

layer is optically thin),

ν_{ij} = frequency of the emitted radiation,

A_{ij} = Einstein transition probability = probability that the atom makes transition i→j spontaneously per second.

The Einstein transition probability, A_{ij}, is related to the f-value by the relation

$$A_{ij} = \frac{8\pi^2 \nu_{ij}^2 e^2}{mc^3} f_{ij}. \qquad (1.3)$$

It is apparent that measurement of the intensity of a spectrum line in an optically thin plasma will yield a value for the product $N_i f_{ij}$, from which the density N_i may be determined if the parameter, f_{ij}, is known.

Many methods have been tried to experimentally determine the f-value of important spectrum lines, an excellent review having been given by Foster (Fo 64). In such a determination, again the quantity $N_i f_{ij}$ is actually measured, but here f_{ij} is determined from the known value of N_i. Most of the difficulties in such measurements are concerned with the determination of N_i to a sufficient accuracy. In the review by Foster, various methods of measuring N_i are discussed, but only for the case of neutral atoms. In stellar spectra, lines are found for atoms having several degrees of ionization. To produce these lines in the laboratory requires some violent excitation such as an electrical spark, and an accurate determination

of the population of the various levels, N_i, becomes impossible. Precise f-values for highly-ionized lines have thus been unobtainable in the past, and the astrophysicist was obliged to use theoretical values, calculated from atomic wavefunctions according to Eq. (1.1) above.

Recently a method has been developed which avoids the necessity of knowing the population, N_i, of the emitting level. In this method the f-value is not measured directly, but is inferred from the related quantity, the radiative lifetime. The relationship between the lifetime, τ, and the f-value may be seen as follows:

Suppose a level, i, has a probability of making a transition per second to another level, j, given by A_{ij}, then $dN_i = -N_i A_{ij} dt$ for the transition i→j. Summing over all possible transitions from level i,

$$dN_i = -N_i \Sigma A_{ij} dt$$

therefore,
$$N_i = N_{io} e^{-\Sigma (A_{ij} t)} . \qquad (1.4)$$

N_{io} being the population of level i at t = 0. The population of the emitted radiation, and hence of the intensity of the emitted radiation, thus falls to 1/e in a time given by $1/\Sigma A_{ij}$. This time is called the radiative lifetime, τ,

i.e.
$$\tau = 1/\Sigma A_{ij} = \frac{mc^3}{8\pi^2 e^2} \cdot \frac{1}{\Sigma (\nu_{ij}^2 f_{ij})} \qquad (1.5)$$

If one of the transitions is dominant, this reduces to

$$\tau = 1/A_{ij} = \frac{mc^3}{8\pi^2 e^2 \nu_{ij}^2 f_{ij}}. \qquad (1.6)$$

It is thus apparent that information concerning the transition probability, A_{ij}, or the oscillator strength, f_{ij}, for a transition from a state i to a state j may be obtained from observations of the decay of intensity of the emitted radiation with time.

1.2 Earlier Methods for Measuring Radiative Lifetimes

Lifetime measurements of excited atomic states were first tried by Wein (We 24) in 1924. A fast-moving beam of excited hydrogen atoms was drawn from a hollow cathode, and the mean lifetime was measured by observing the variation of the beam intensity with respect to the distance. No accurate results could be obtained because the location of excitation was not sharply defined. Two major techniques were then developed: the phase shift technique and the delayed coincidence technique.

In the phase shift technique (Ma 29, Ma 31, Br 62, Br 63), the spectrum of interest is excited by exposing the gas or vapour to a sinusoidal exciting signal, which can be a pulsed source of ultravoilet light, of electrons or of protons. The fluorescent light shows a modulation of the same form as the exciting signal with same frequency but is delayed by a phase angle, θ, which is related to the lifetime, τ, by (Br 63, Fo 64)

$$\tan \theta = 2\pi f\tau \qquad (1.7)$$

where f is the frequency of the modulated signal. Therefore the lifetime is measured by observing, with a sensitive oscilloscope, the phase shift between the excitation signal and the fluorescent light.

In the delayed coincidence technique (Kl 66, Ka 67, Ni 68), the excitation and fluorescent signals are fed to a time-to-pulse-height converter. The excitation signal is used to start, and the fluorescent signal to stop, a signal in the converter. The distribution of the fluorescent signal as a function of time is converted to a distribution as a function of pulse height. A multichannel-pulse-height analyzer is then used to analyze and display the results. The mean lifetimes can then be deduced from the distribution curve.

As mentioned before, no accurate data could be expected from Wein's method because the exact place of excitation was not known and the velocities of the atoms were not accurately defined. The accuracy of the phase shift technique is limited by the resolution of the oscilloscope and is seldom as precise as ±1 nsec (Br 62). Delay coincidence has been more commonly used during the last decade (Ka 67). Its accuracy is limited by the time-resolution of the coincidence circuit (≃1 nsec). Both the phase shift and delayed coincidence techniques have the considerable

disadvantage that the measurement of lifetimes for highly ionized atoms is impossible because no such spectrum lines have been excited in fluorescence. A different technique is, therefore, necessary for such measurements.

1.3 The Beam-Foil Technique

That a highly energetic particle beam excited by collision with a thin carbon foil (~10 $\mu g/cm^2$) could be used as a new light source for lifetime measurements was first proposed and performed by Kay (Ka 63). The beam-foil excited atoms give off light while decaying spontaneously to their ground states. Since the velocities of the atoms are uniform, a study of the decay of the brightness of the beam will give the mean lifetimes of the excited states. Kay employed a Raman spectrograph to observe the nitrogen spectrum. The resolution was poor and only 13 lines, at the wavelength range 4000-5000 Å, were obtained. Bashkin et al. (Ba 65, Ba 66a, Bi 66, Bi 67a, Bi 68) developed the beam-foil technique further and observed the mean lifetimes and the dependence of spectral line intensity upon beam energy using hydrogen (Bi 68), deuterium (Ba 66a), helium (Bi 67b), neon (Ba 64, Ba 66b), and nitrogen (Fi 68). Qualitative observations have also been made for oxygen (Ba 66a).

The most important feature of the beam-foil technique is that the place of excitation of all the particles is exactly located and defined to an infinitesimal

interval. With the carbon foil of thickness 10 $\mu g/cm^2$, the time required for the beam particles to traverse the foil is of the order of 10^{-15} sec. This precisely known location of excitation and the uniform velocity of the beam particles make the beam-foil technique the most elegant as well as straightforward method for lifetime measurements.

Another advantage of the beam-foil technique is that multiply-ionized atoms are easily obtained. Besides serving as an exciter, the carbon foil also serves as an electron stripper. Highly ionized atoms can be obtained by increasing the thickness of the foil. Nevertheless, thick foils are not preferred because all degrees of ionization are equally interesting. In comparison to the traditional light source, the beam-foil excitation source is extremely pure and easy to control.

An analyzing magnet can be used, which will allow only isotopically pure, monoenergetic and unidirectional particles to bombard the carbon foil and thus only the spectrum from atoms of the same mass and velocity will be detected. Also, the intensity can be controlled by varying the beam current. In most cases, however, it is advisable to use the maximum possible intensity.

It may also be noted that due to the particular nature of the beam-foil technique, the Doppler shift can be experimentally verified. Another point is that an evacuable spectrometer can be connected directly to the vacuum chamber.

The lack of any medium between the light source and detector makes the study of the extreme ultraviolet spectrum region possible. The ultraviolet region is particularly important for highly ionized atoms. Space physics has made the detection of the extreme ultraviolet from the sun and stars possible. To analyse the data, i.e. to identify the spectrum lines, laboratory ultraviolet observations are badly needed, and the beam-foil technique can be most useful in this regard.

1.4 Lifetime Measurements Using the Beam-Foil Technique

After being excited by collision with the foil, the beam particle will decay. Neglecting repopulation of the upper level by cascade transitions, the decay will take place according to the equation:

$$N(t) = N_o e^{-\alpha t} \tag{1.8}$$

where N_o is the number of atoms in the initial state excited by traversing the foil, N(t) is the number of atoms in this state remaining undecayed, α is the decay constant and is the probability per unit time that the excited state will decay. If the speed of the particles is v, and the distance from the foil on the down stream side of the foil is x, then

$$N(x) = N_o e^{-\frac{\alpha x}{v}}. \tag{1.9}$$

Therefore, if the Einstein coefficient is designated A_{ij}

then the detected signal, I(x), will be

$$I(x) = kA_{ij}N_o e^{-\frac{\alpha x}{v}} \tag{1.10}$$

where the constant, k, depends on geometrical factors and detection efficiency of the spectrometer and photomultiplier. Suppose several final states are possible, the decay constant, α, is by comparision with Eq. (1.5)

$$\alpha = \Sigma_j A_{ij} = 1/\tau. \tag{1.11}$$

Therefore, Eq. (1.10) can be written as

$$I(x) = kA_{ij}N_o e^{-\frac{x}{\tau v}}. \tag{1.12}$$

A semilogarithmic plot of the intensity against the distance from the foil will thus result in a straight line, from which the lifetime of the initial state can be deduced. Fig. 1.1 is a typical intensity plot.

In cases where repopulation of the upper level by cascade transitions is important, the result will be more complicated to interpret. Let the states be designated k, i, j as shown in Fig. 1.2, then

$$dN_i = A_{ki}N_k dt - N_i \alpha_i dt \tag{1.13}$$

where $\alpha_i = \Sigma_j A_{ij}$. If level k is not in turn fed by higher cascade processes, then we may write

$$N_k = N_{ko} e^{-(\alpha_k t)} \tag{1.14}$$

where $\alpha_k = \Sigma_i A_{ki}$. Hence, the solution to Eq. (1.13) is

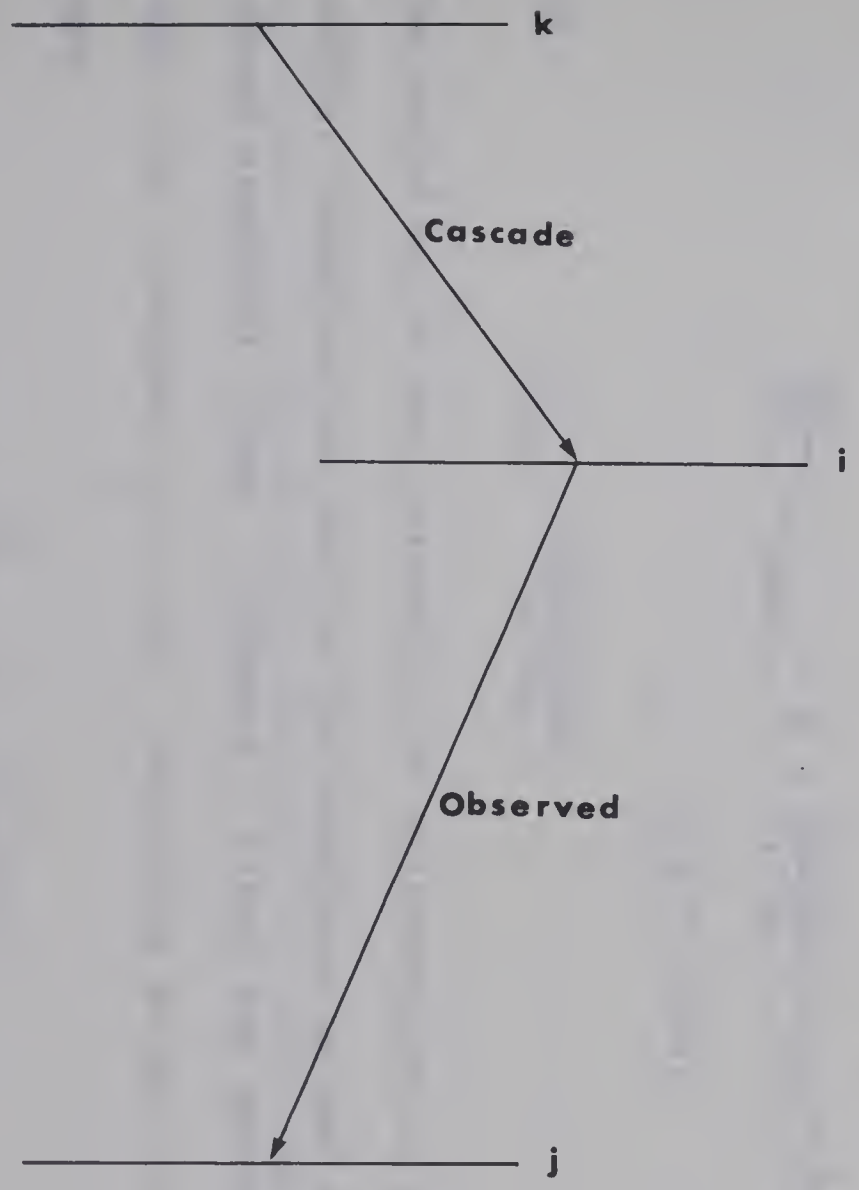

FIG. 1.2 Diagram for a cascade transition.

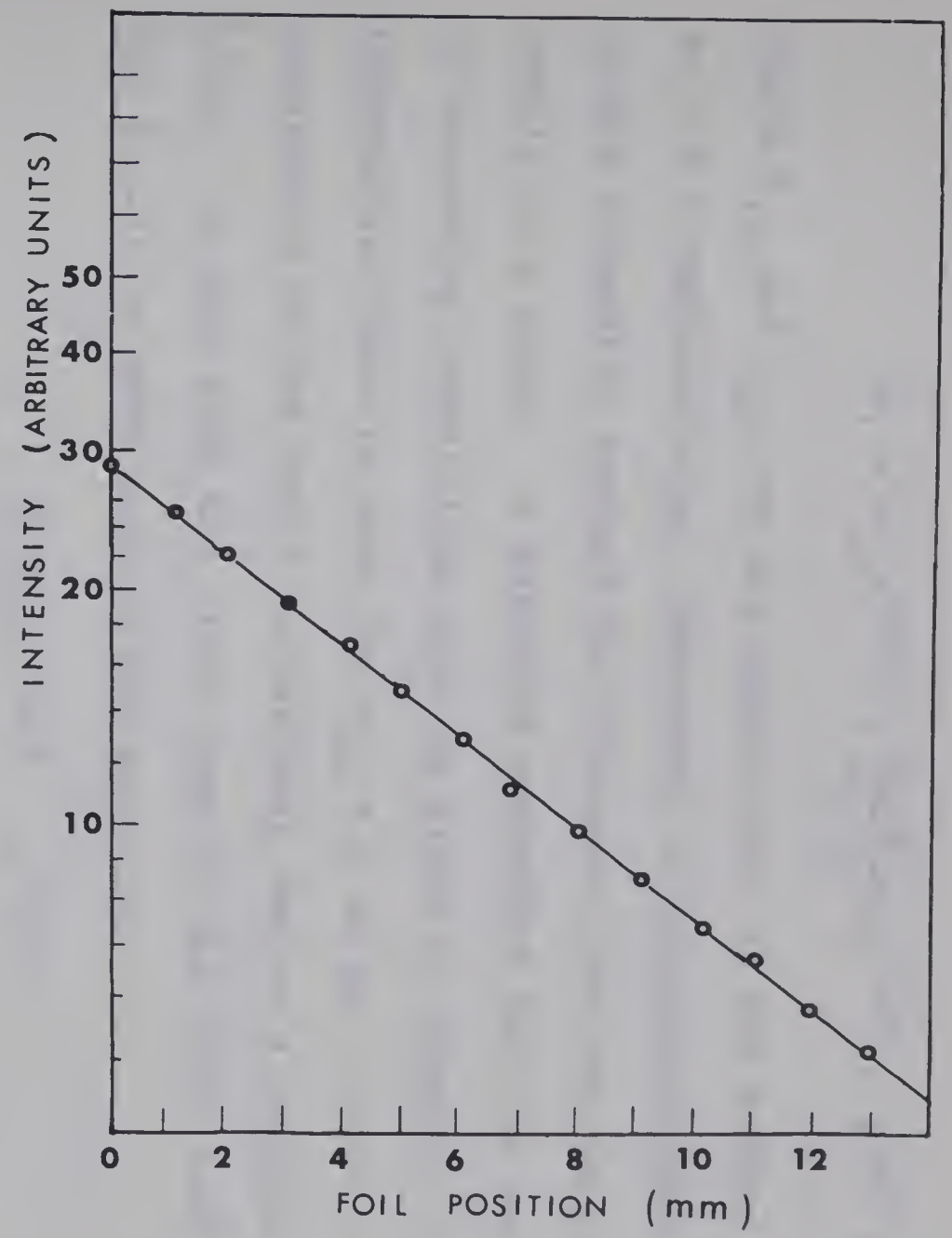

FIG. 1.1 Semilogarithmic plot for O–4374.

$$N_i = N_{io}e^{-\alpha_i t} + \frac{A_{ki}N_{ko}}{\alpha_i-\alpha_k}(e^{-\alpha_k t} - e^{-\alpha_i t}) \quad (1.14)$$

where N_{io} and N_{ko} are the populations of the states i and k at t = 0 respectively. Therefore, a semilogarithmic plot of the intensity against the distance from the foil will result in a curve. A detailed procedure for the analysis of cascading transitions will be given in Chapter III. An interesting case is that for $N_{io} = 0$ in Eq. (1.14), i.e. the population of the state is entirely due to a cascade transition. In this case the first term on the right hand side of Eq. (1.14) is zero leaving the equation

$$N_i = \frac{A_{ki}N_{ko}}{\alpha_i-\alpha_k}(e^{-\alpha_k t} - e^{-\alpha_i t}) \quad (1.15)$$

Therefore the intensity is zero at t = 0 and t = ∞. Hence N(t) must rise to a maximum value at time, t_{max}, given by

$$\left(\frac{dN_i}{dt}\right)_{t=t_{max}} = 0 = \frac{A_{ki}N_{ko}}{\alpha_i-\alpha_k}(-\alpha_k e^{-\alpha_k t_{max}} + \alpha_i e^{-\alpha_i t_{max}}) \quad (1.16)$$

or
$$t_{max} = \frac{\ln(\alpha_i/\alpha_k)}{\alpha_i-\alpha_k} \quad (1.17)$$

The build up of the intensity is illustrated in Fig. 1.3. Another complication met in the analysis is due to unresolved spectral lines. Suppose n lines are unresolved, each with lifetime $\tau_i = 1/\alpha_i$, according to Eq. (1.10) we have

$$I(x) = \sum_i^n kA_{ij}N_{io}e^{-(\alpha_i x/v)} \quad (1.18)$$

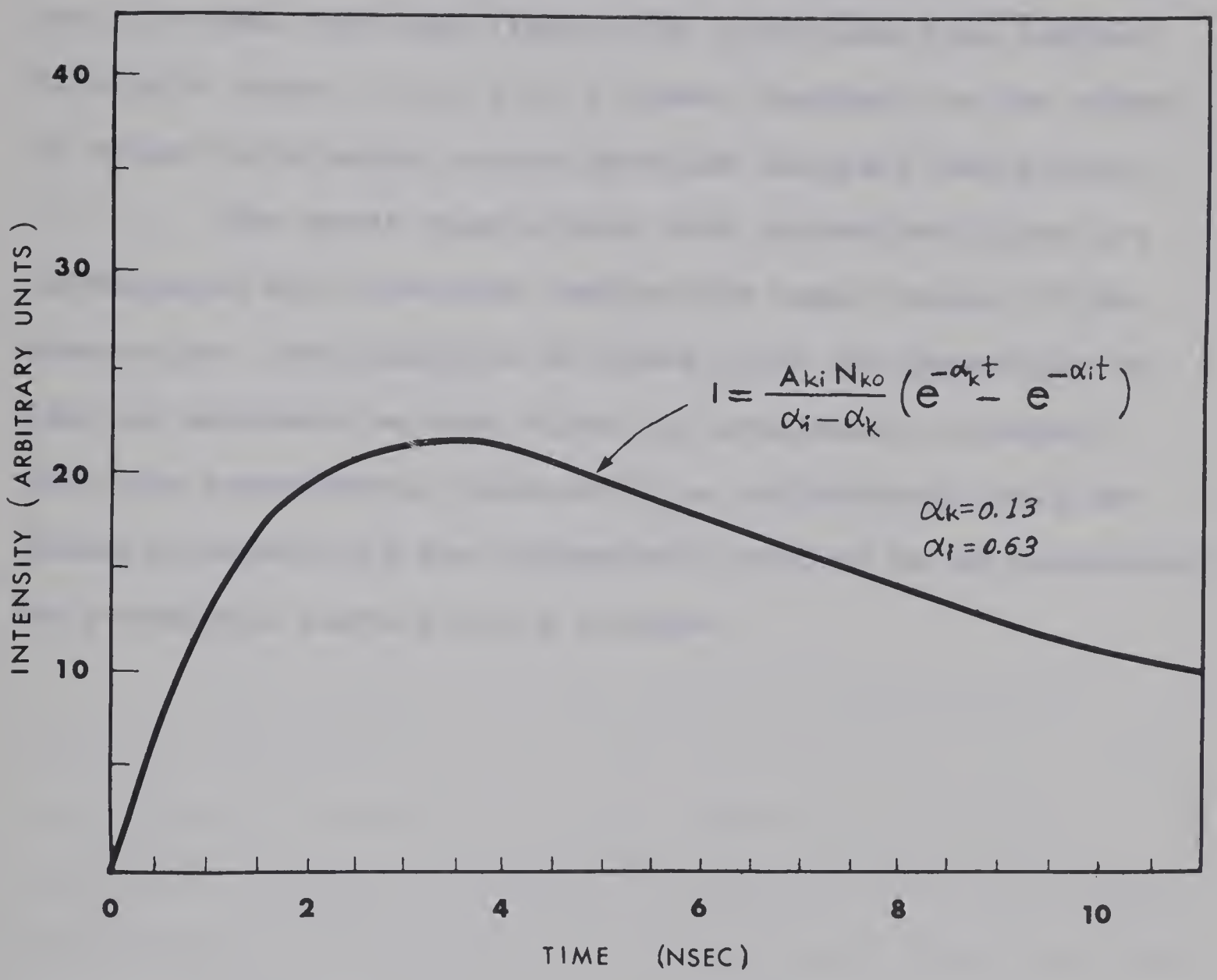

FIG. 1.3 Growth and decay of a cascade populated state.

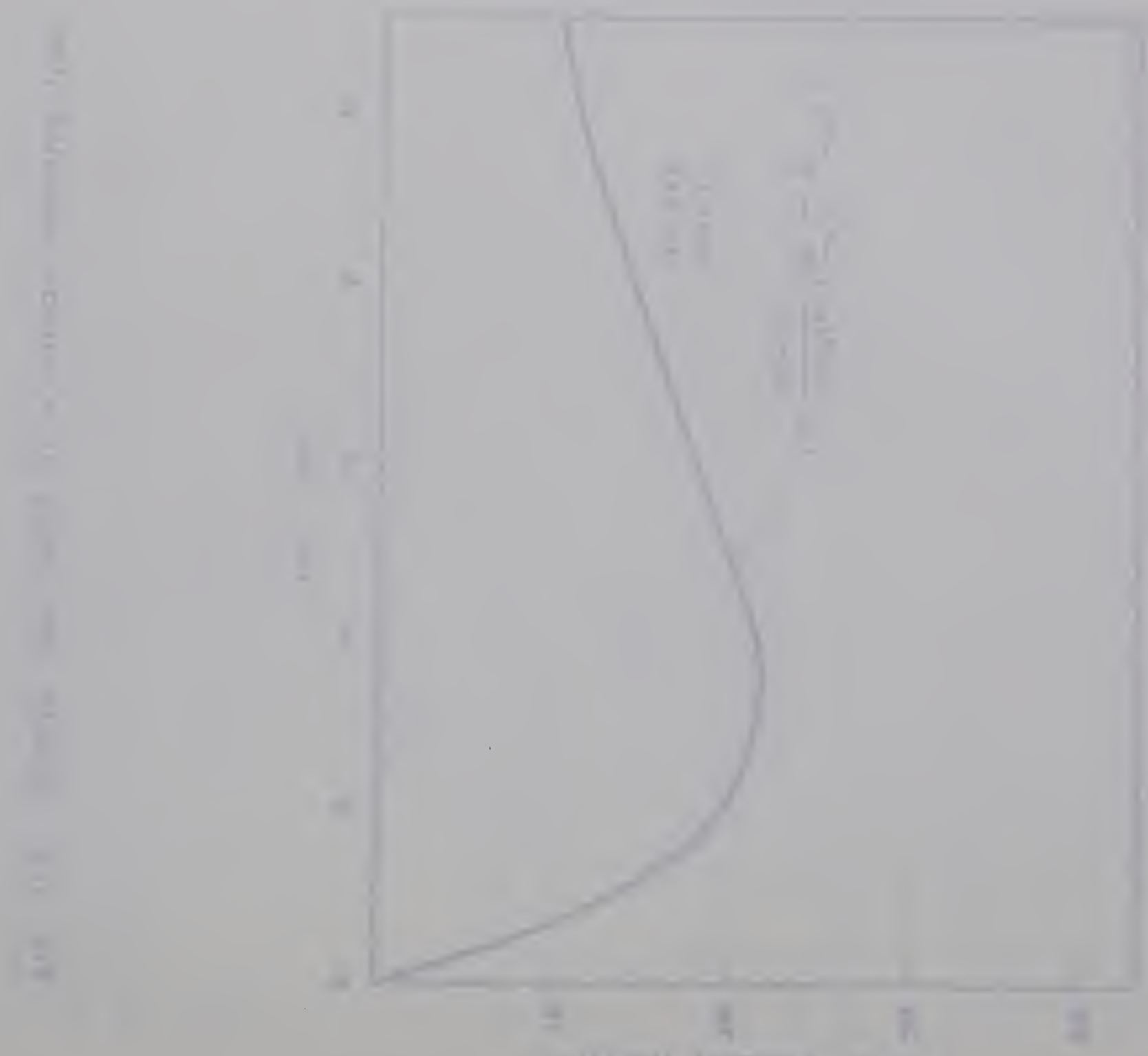

The resulting decay curve would then be the composition of n straight lines with different slopes. In principle, a curve-fitting computer program can be employed to determine the lifetimes for each lines, but this should be limited to simple cases, i.e. 2 or 3 lines, because the low signal to noise ratio makes a more detailed analysis impractical.

The worst case occurs when unresolved lines are accompanied with cascades feeding the upper states of the transition. The analysis of these lines is impossilbe unless an extremely strong signal is available, in order that the experimental curve will be sufficiently well defined to permit all the parameters involved to be determined by a computer curve-fitting program.

CHAPTER II

EQUIPMENT

2.1 Introduction

The beam-foil excitation technique requires a source of ions travelling at velocities of the order of 10^8 cm/sec. The most suitable device to achieve such a beam velocity is a Van de Graaff accelerator capable of handling positive ions at energies of the order of 1 MeV. Such a machine was made available by the Committee on Radiation Research and thus this project became possible. The success of these experiments is largely due to the enthusiastic assistance of Mr. E. B. Cairns of the Radiation Research Laboratory.

The work normally performed in the Radiation Research Laboratory requires the accelerator to be operated as an electron machine. A fairly complex conversion is required to change the machine to a positive ion accelerator. During the last two years, two sets of experiments have been performed. In the first case, the machine was made available for four weeks around September 1967. Of these four weeks, ten days were actually used in the experiment, the rest of the time being necessary to affect the conversion to a positive ion machine. In the second run, which was made in June 1968, the conversion was made more quickly, giving two full weeks for observation. In the description of the equipment which follows, items used in the first set of

experiments will be indicated by (1967) and those in the second set by (1968).

The equipment used in these experiments consisted of the following items:

a) the Van de Graaff accelerator and its subsidiary equipment,

b) the target chamber and optical focusing devices,

c) the spectrometer and photomultiplier.

A description of each of these items and the criteria which they had to satisfy now follows. The general arrangement is shown schematically in Fig. 2.1.

2.2 The Van de Graaff Accelerator and Subsidiary Equipment

The Van de Graaff accelerator used in these experiments (Fig. 2.2) was Model AK 60 from the High Voltage Engineering Corporation, which would supply accelerating voltages from 0.5×10^6 volts to 2×10^6 volts. An ion source of the usual radio-frequency discharge type was located at the high voltage terminal. For the experiments to be described in this thesis, the ion source bottle was filled with 99.99 % pure oxygen from Matheson of Canada, Ltd. The source produced a supply of singly charged atoms and molecules as well as doubly charged atoms. However the largest component by far is singly charged molecules, O_2^+, and hence this component was used. The molecules are, of course, disso-

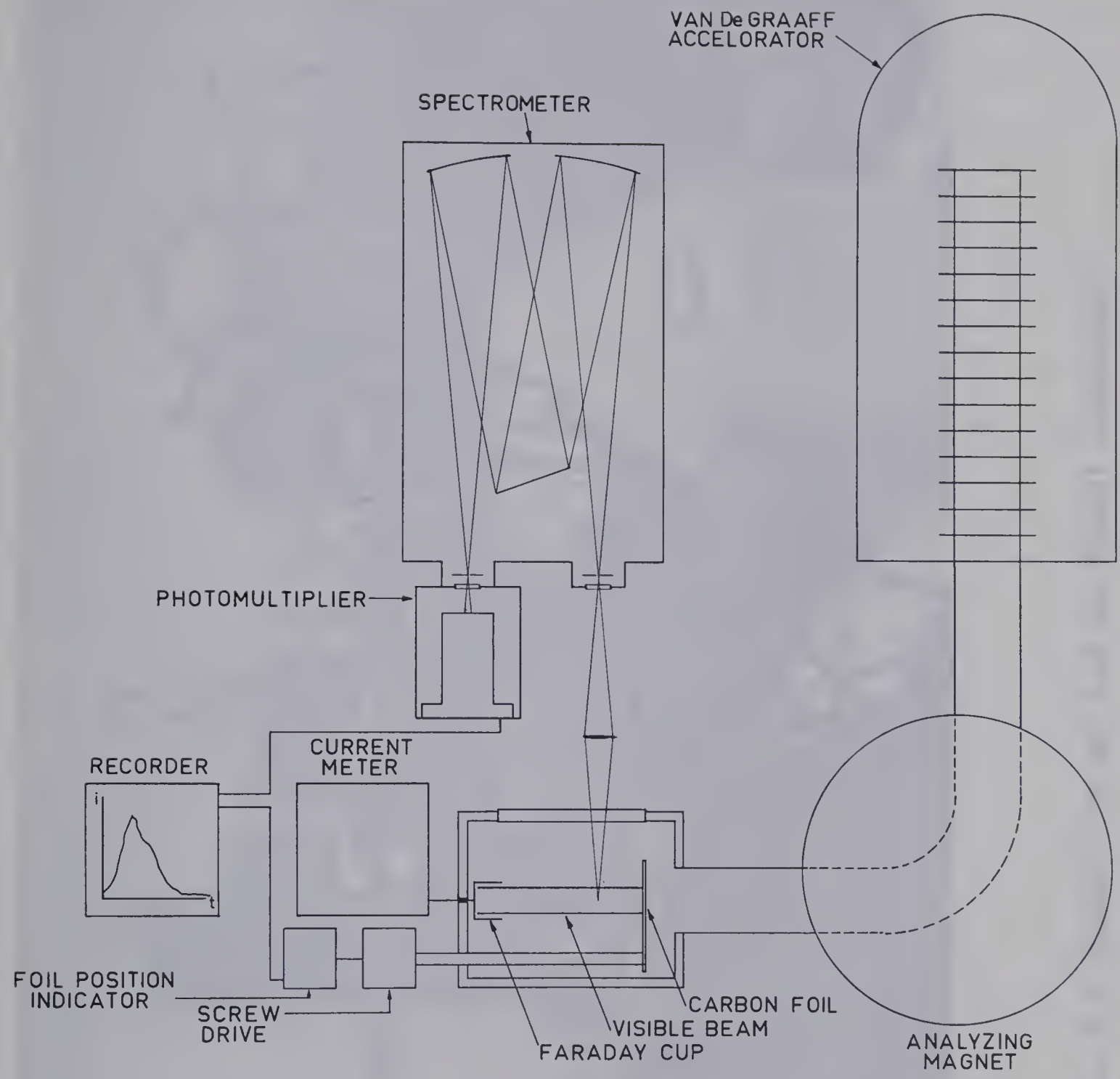

FIG. 2.1 Schematic diagram of the basic principle of the ion beam technique.

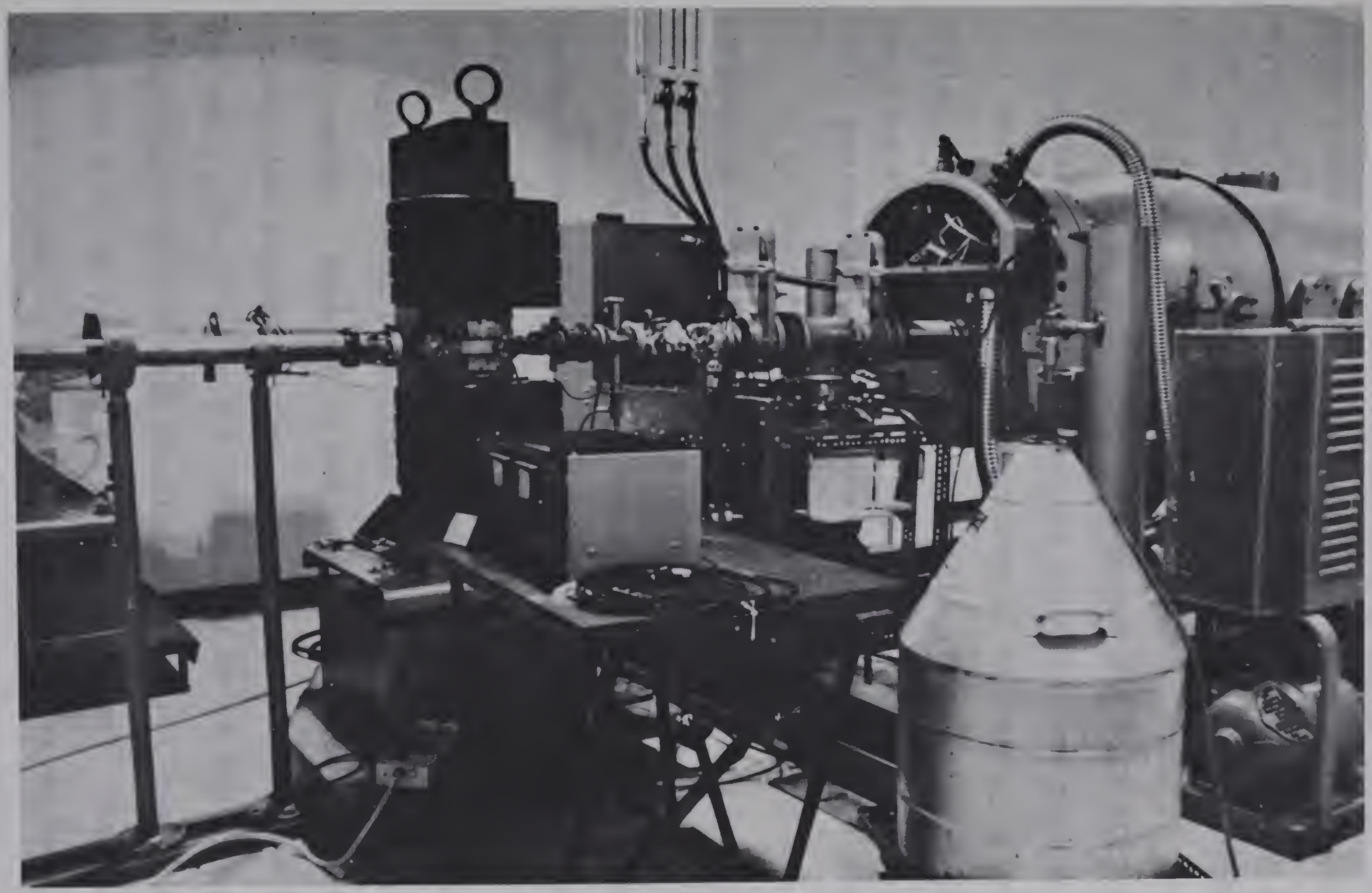

FIG. 2.2 Model AK 60 Van de Graaff accelerator.

ciated in passing through the carbon foil, producing two atoms travelling at almost the same velocity as the incident molecule. There is an energy loss of about 8% for 1 MeV O_2^+ ions incident on 10 $\mu g/cm^2$ foil, as will be described in Section 3.2.

It is necessary to bombard the foil with only one of the various species emerging from the ion source as they will each produce ions travelling at different velocities. Neglecting energy loss in the foil, the ions produced from the parent particles O_2^+; O^+ or O_2^{++}; O_2^{+++}; and O^{++} or O_2^{++++} would possess velocities in the ratios $1:\sqrt{2}:\sqrt{3}:2$ respectively. It is therefore necessary to select one of the beam components before the beam reaches the foil. A horizontal analyzing magnet from the High Voltage Engineering Corporation was available in the Radiation Research Laboratory. The maximum mass-energy product which this magnet would bend through 25° was about 8 (the mass-energy product is expressed in units of a.m.u.xMeV). For O_2^+ at 1 MeV the mass-energy product is about four times that which could be handled by this magnet. However it was possible to send the beam through the magnet chamber slightly off-center and to arrange the exit pipe at an angle of about 3.5° to the incident direction. It was then possible to deflect the O_2^+ beam through 3.5° on passing through the magnet. That this deflection is sufficient to separate the various beam components may be seen from the following calculation. The de-

flection produced by a magnet is given by the relation

$$R = \frac{1}{B}\sqrt{2Vm/Q} \qquad (2.1)$$

where R = radius of circular orbit of particle while inside the magnetic field B,

V = accelerating voltage through which the particle of mass m and charge Q has passed prior to entering the magnet.

The other significant component of the ion beam was O^+. From Eq. (2.1) it is apparent that, for the same magnetic field B,

$$\frac{R(O_2^+)}{R(O^+)} = \sqrt{2}\ . \qquad (2.2)$$

If the length of the path inside the magnet chamber is ℓ,

then $$R(O_2^+)\Theta(O_2^+) = R(O^+)\Theta(O^+) = \ell \qquad (2.3)$$

where $\Theta(O_2^+)$ and $\Theta(O^+)$ are the deflections produced in passing through the magnet for O_2^+ and O^+ particles respectively.

Hence $$\Theta(O^+) = \Theta(O_2^+)\frac{R(O_2^+)}{R(O^+)} = \sqrt{2}\Theta(O_2^+). \qquad (2.4)$$

Thus for an O_2^+ deflecting of 3.5°, a deflection of 5° may be expected for O^+ particles. The separation of O_2^+ and O^+ thus is about 1.5°, or a spatial separation of about 2.5 cm for every meter of beam pipe.

The ion beam was collimated by a diaphragm with an aperture of 0.25 in. placed immediately before the target

chamber. It was found that for foils of thickness 25 $\mu g/cm^2$ (1967), the beam current had to be maintained at less than 1 μA in order for a foil to last more than a few seconds. Consequently beam currents of 0.35 μA were used, except for very faint spectrum lines, where the current was increased to 0.5 μA. Foils of thickness 10 $\mu g/cm^2$ (1968) were found to be more durable and beam currents of around 1 μA were used.

2.3 The Target Chamber and Focusing Device

Three functions need to be performed by the target chamber and focusing device:

a) the ion beam (in this case O_2^+) from the accelerator must be made to strike a suitable carbon foil,

b) the light emitted by the ions after passing through the foil must be focused on the spectrometer slit,

c) the image of the beam must be scanned across the spectrometer slit in a controlled manner if the decay of intensity with distance from the foil is to be determined.

Two different arrangements were attempted to meet these requirements and these are shown in Figs. 2.3 and 2.4.

In the first arrangement, used in September 1967, the target chamber simply consisted of a brass chamber fitted

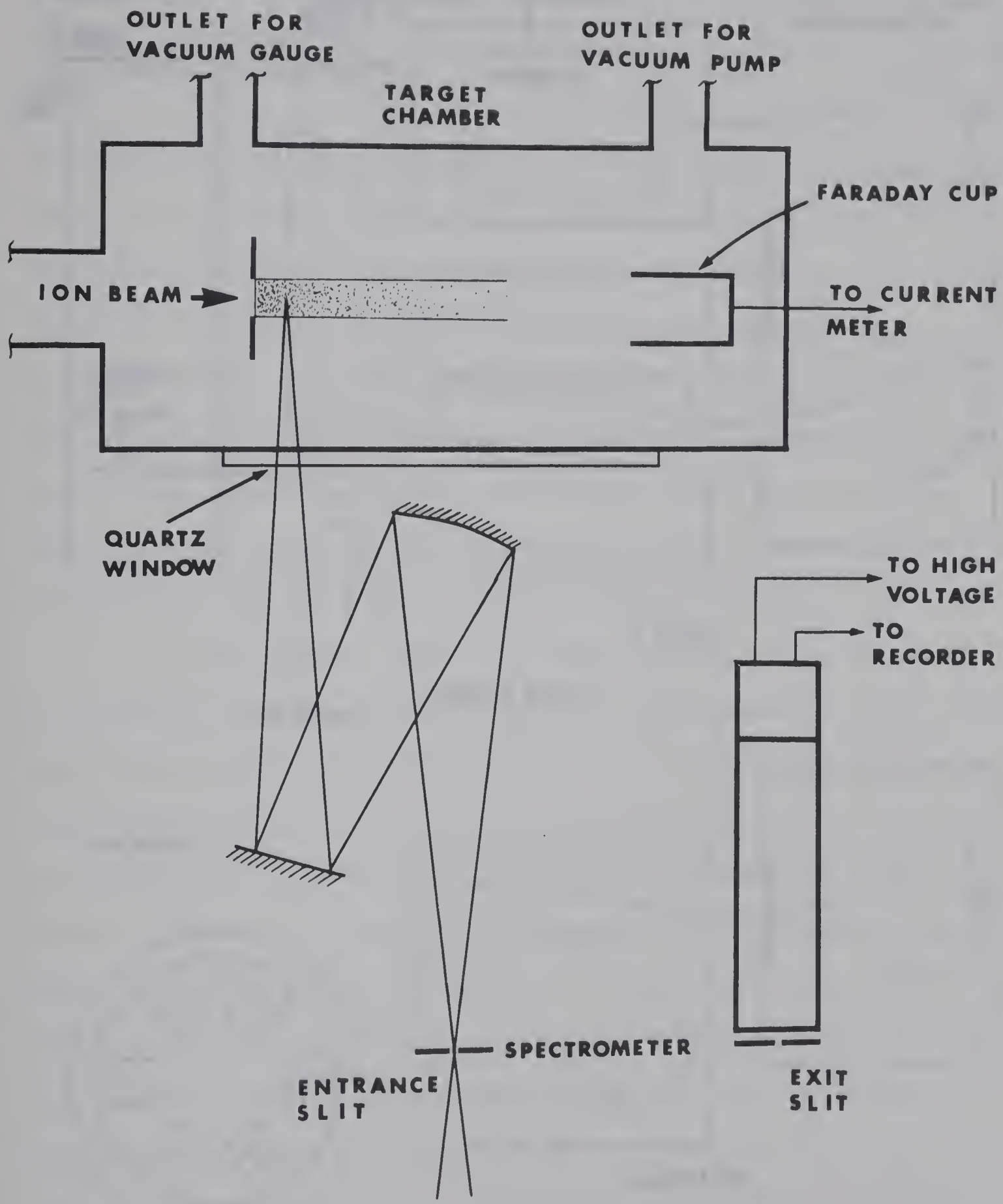

FIG. 2.3 First experimental arrangment (schematic only).

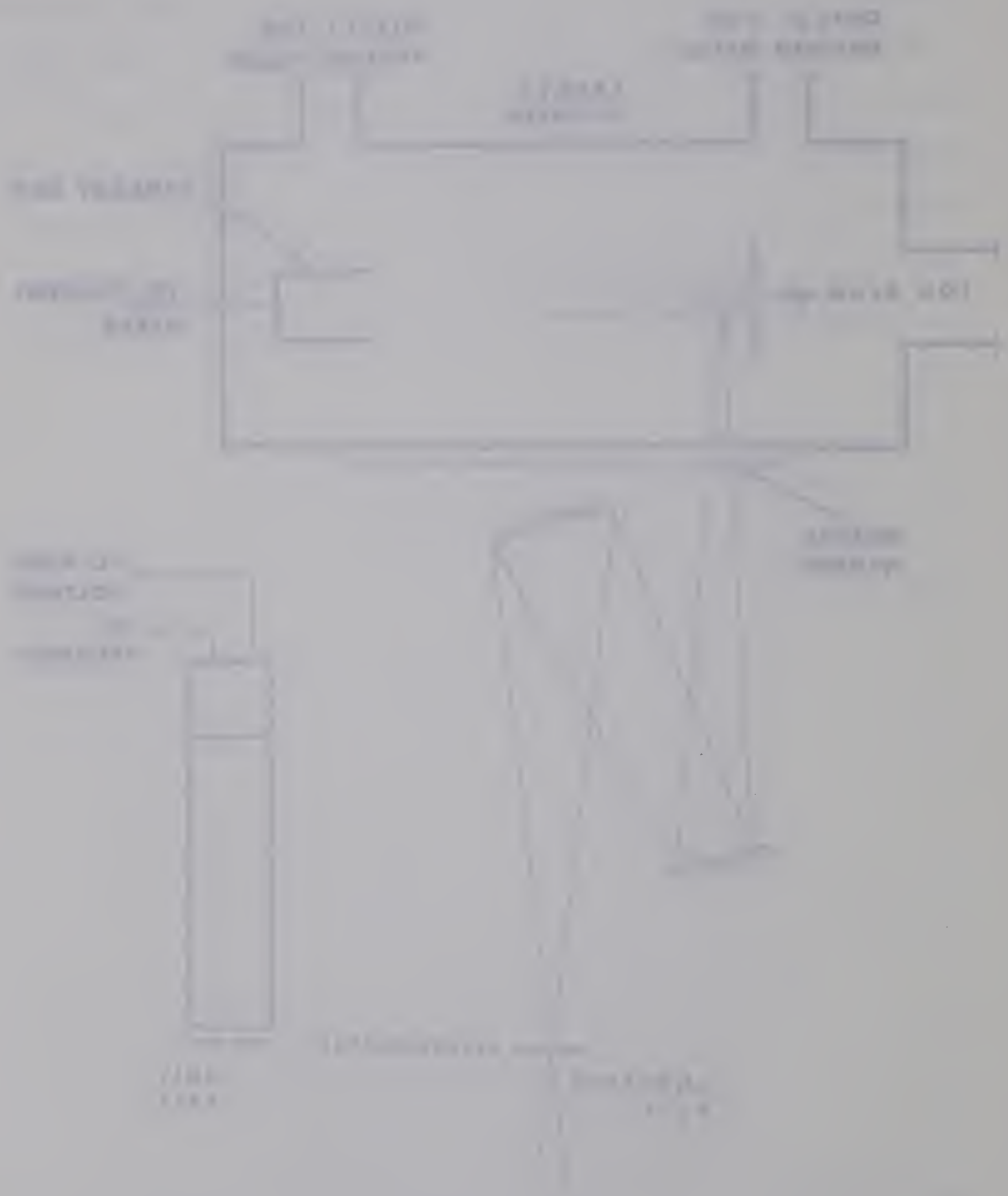

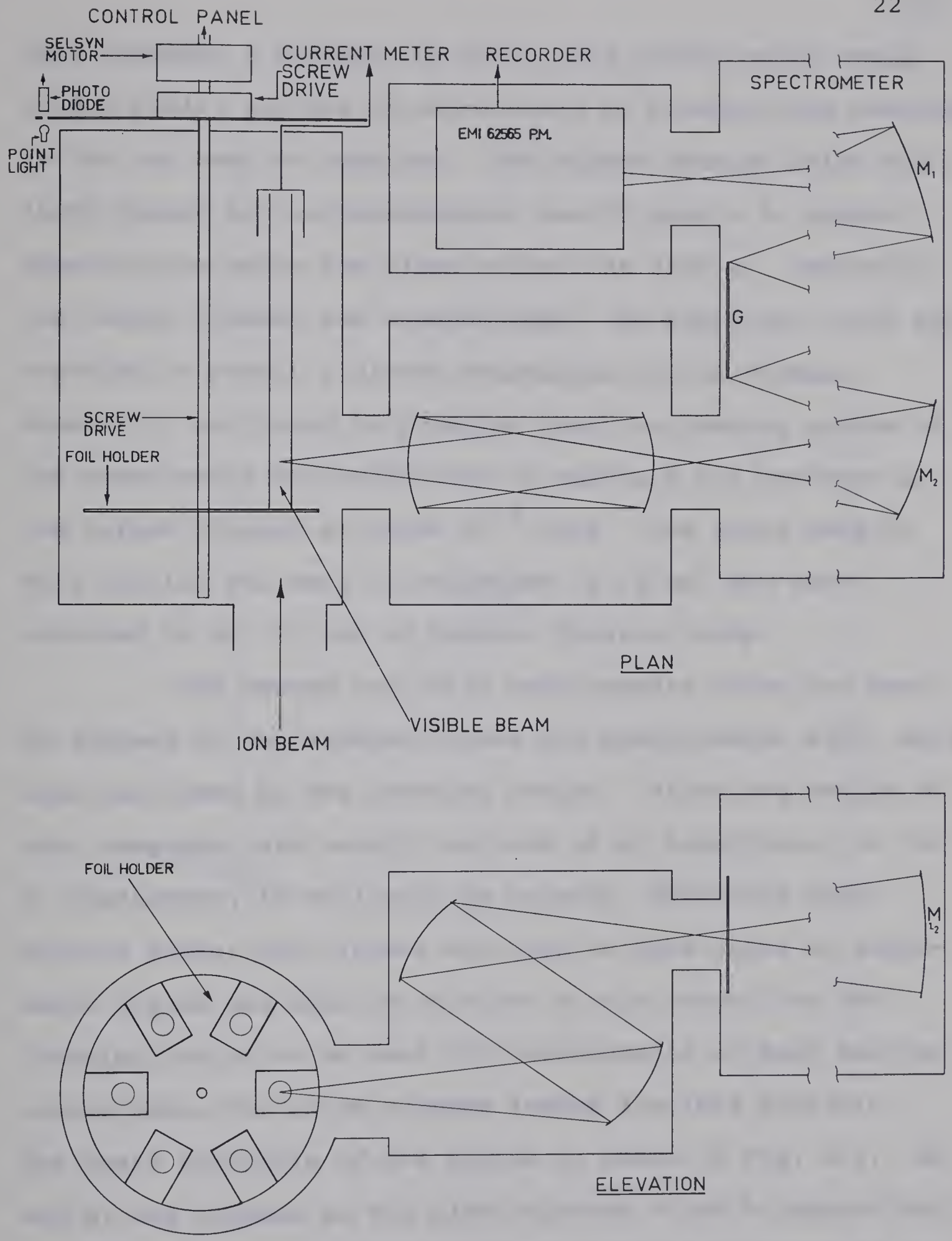

FIG. 2.4 Second experimental arrangement (schematic only).

with windows, a Faraday cup and a foil holder which would hold 6 foils, any one of which could be brought into position in the ion beam as required. The window through which the light passed to the spectrometer was of quartz to permit observations below the glass cut-off at 3500 Å. Naturally the target chamber was vacuum-tight. An auxiliary inlet was provided to permit a direct evacuation of the chamber. However it was found in practice that the pumping system of the accelerator was sufficient to maintain the pressure in the target chamber at below 10^{-5} torr. The foils used in this initial run were of thickness 25 $\mu g/cm^2$ and were provided by Dr. G. Roy of Nuclear Physics Group.

The second and third requirements, that the beam be focused on and scanned across the spectrometer slit, were both performed by the focusing device. Since the design of this component was mainly the work of my supervisor, Dr. E. H. Pinnington, it will only be briefly described here. Mirrors rather than lenses are used as this gives an achromatic system and also as this was a trial model for the focusing device to be used for measurements at much shorter wavelengths, for which purpose lenses are less suitable. The basic principle of the device is shown in Fig. 2.5. AX and BY are normals to the plane mirrors A and B respectively. Mirror A is able to move along MN in such a way that AX always points towards C, such that AB = BC. The mirrors A and B are then mechanically connected so that AX is always

FIG. 2.5 Basic principle of the focusing device.

parallel to BY. The result of constructing the device in this way is that wherever mirror A is along MN, light leaving the ion beam in a direction perpendicular to the beam will strike mirror A, then B and finally pass along the line BS, which is made the optical axis of the spectrometer. It is necessary that the light reaches the spectrometer should leave the ion beam perpendicularly to avoid a Doppler effect wavelength shift. A fixed speed servo motor was used to drive the mirror along the line MN at a known rate. This together with the known rate of paper advance on the chart recorder, sufficed to correlate distance on the chart paper with distance from the foil along the beam. Thus the required scanning action was achieved. Focusing was obtained by replacing one of the mirrors with a suitable concave mirror. In practice a concave mirror of focal length 25 cm was used. Naturally, using a concave mirror off-axis in this manner produced noticeable astigmatism. It was therefore necessary to use the horizontal focus. The vertical astigmatic image was then only a few mm, and as the beam image itself was about 1 cm, and the length of the spectrometer slit is 2 cm, this small amount of astigmatism was not serious.

In the second set of experiments (1968), it was hoped to extend the range of observation down to the limit of the spectrometer at 1100 Å. To this end a new target chamber and focusing device was constructed, as shown in Fig. 2.4.

Here the scanning was performed inside the target chamber by moving the foil itself. Again the foil holder held 6 foils at a time, and each could be used in turn. The foils used in 1968 experiments had thickness of 10 ± 4 $\mu g/cm^2$, mostly obtained from Yissum Research Corp. but, when this supply proved insufficient, some additional foils were provided by Dr. G. Roy. The drive screw for scanning the foil had a 1 mm pitch, so that 1 revolution corresponded to moving the foil by 1 mm. An indicator wheel was mounted on the driving shaft but outside the chamber itself. By means of a small bulb, and a hole in the wheel, an electric signal was obtained once per revolution of the wheel and hence once for every advance of the foil by 1 mm. These pulses were fed to the side-event marker on the chart recorder. Also connected to the driving shaft was one of a pair of Selsyn motors. The other Selsyn motor was mounted on the control panel situated in the accelerator control room, and was made to drive a simple counter. In this way the position of the foil inside the chamber was known at all times by the operator in the control room. The foil drive screw was also fitted with limit switches to prevent the foil holder being driven too far in either direction. The motor for turning the drive screw was a Model 2J6FA3 from Canada General Electric Co. Ltd. This motor was variable in speed from 10 to 100 RPM. It was not necessary to know the exact speed of the motor as the foil position was recorded in the chart

by the photodiode mentioned above.

The focusing device, again designed by Dr. E. H. Pinnington, used the same optical principle as the 1967 version, i.e. an out-of-plane concave and plane mirror combination. For the observations below 2000 Å, a pair of MgF_2 overcoated aluminum mirrors were used, and above 2000 Å, a pair of SiO_2 overcoated aluminum. No windows were used between the ion beam and the spectrometer slit. The vacuum was thereby maintained from the accelerator through the target chamber to the focusing chamber. Since the mirrors were inside a sealed chamber, it was necessary to adjust their alignment by means of controls which passed through the chamber wall but were nevertheless vacuum tight. Two controls were actually used. The first adjustment was designed to move one of the mirrors to and fro without changing its spatial orientation. This permitted fine adjustments to be made to the object and image distances to obtain the optimum focus. The second adjustment was designed to rotate the other mirror about a horizontal axis through its surface. A MgF_2 window was used at the spectrometer slit so that the vacuum in the spectrometer could be maintained when the target chamber was opened for the purpose of replacing foils etc.

A further experiment in the 1968 set was made to actually measure the velocity of the particles in the beam directly. For this purpose the 1967 target chamber was

modified as shown in Fig. 2.6. Two small front-surface mirrors, M_1 and M_2, were introduced inside the chamber, so arranged to reflect light from a portion of the beam just in front of the foil, M_1 reflecting light at 30° to the beam, and M_2 at 10° to the beam. Thus three beams were obtained:

A at 90° to the beam direction,

B at 30° to the beam direction,

C at 10° to the beam direction.

These beams were focused consecutively on the spectrometer slit by the 1967 focusing device described earlier.

2.4 The Spectrometer

The spectrometer used throughout these experiments was an f/6.8 Model 1500, 0.75 meter in-plane Ebert type spectrometer from Spex Industries, containing gratings having 1200 grooves per mm, and blazed for 5000 Å (for measurements above 3000 Å) or for 1500 Å (for measurements below 3000 Å). The first order dispersion was about 10 Å/mm. The instrument was fitted with a wavelength counter which was accurate to ±1 Å, and a wavelength marker which gave a signal pulse every 5 Å. This pulse was fed to the side-event marker on the chart recorder and used to identify the wavelengths of the lines in the beam-foil excited spectrum.

The signals obtained were extremely low. It was therefore necessary to use a slit somewhat wider than would normally be used. The slit width was set at 0.4 mm,giving

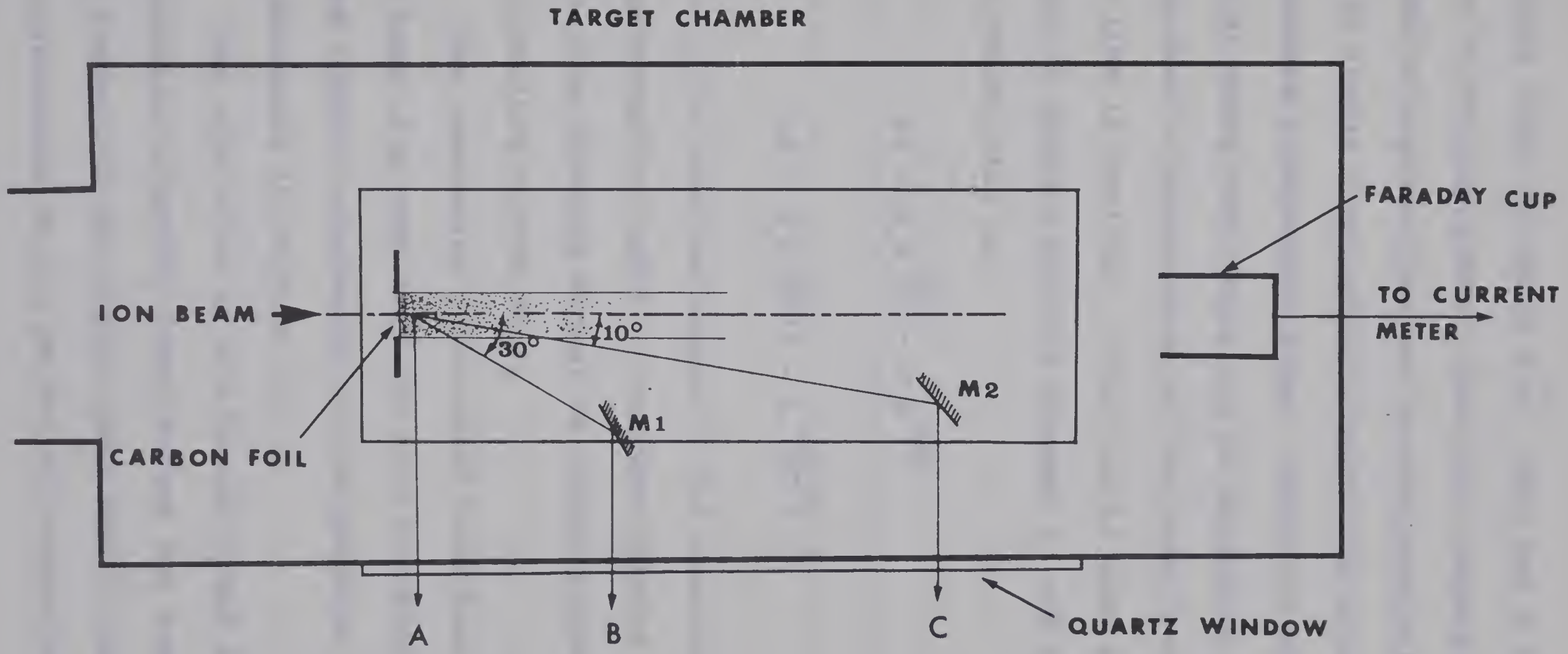

FIG. 2.6 Target chamber for beam velocity measurements.

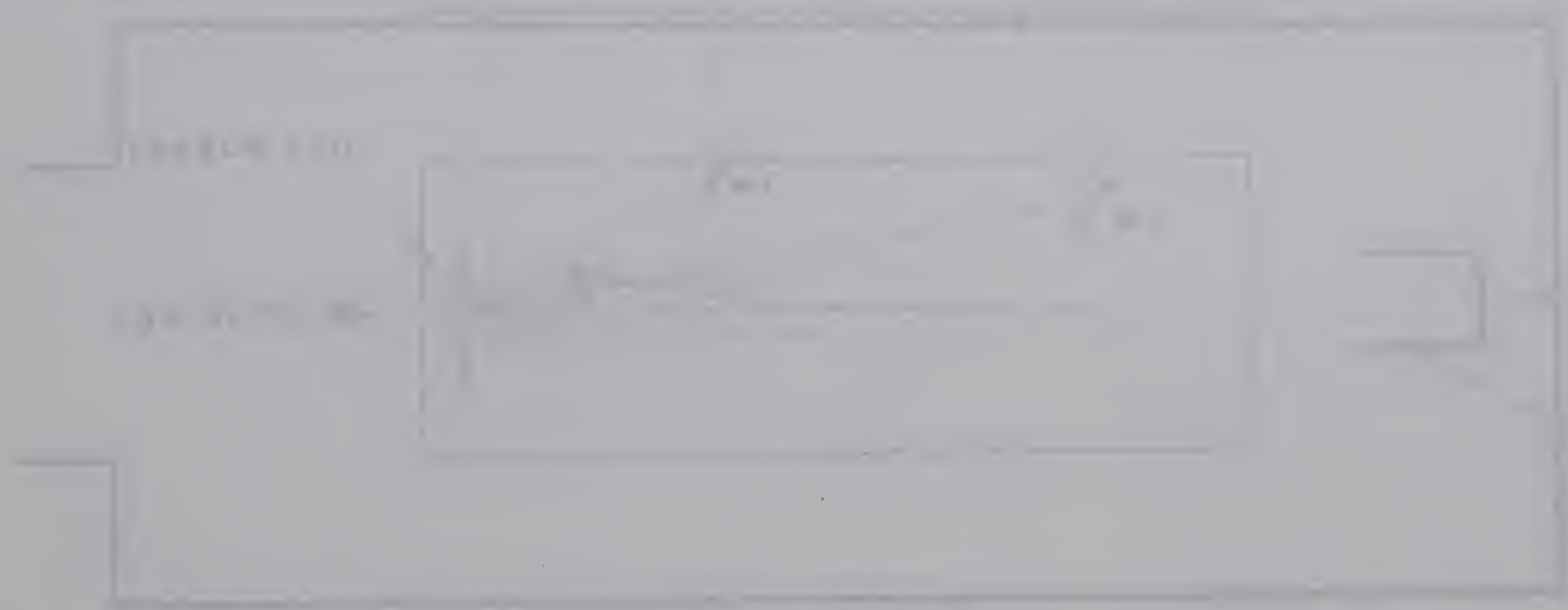

a resolution limit of about 4 Å. This was a source of uncertainty in the experiment, both with regard to the exact wavelength of a given line and to the possibility of an apparently single line actually being two or more overlapping but unresolved independent lines. Having a wide slit, the exponential decay rate would not be distorted through averaging over a long section of the beam if only a single spectrum line is admitted. This can be seen by considering the number of photons emitted between ℓ_1 and ℓ_2 from the foil, ΔN, which will be

$$\Delta N = N_o e^{-\frac{\ell_1}{v\tau}} - N_o e^{-\frac{\ell_2}{v\tau}} \qquad (2.5)$$

or

$$\Delta N = N_o e^{-\frac{\ell_1}{v\tau}}(1 - e^{-\frac{\ell_2-\ell_1}{v\tau}}). \qquad (2.6)$$

Now, $\ell_2 - \ell_1$ is just the length of the beam which was imaged to the spectrometer, and is a constant during a measurement. Therefore, the observed signal is simply proportional to the number of excited states at ℓ_1.

The resolution limit would have been approximately the same even if a much narrower slit had been used. This is due to the Doppler broadening of the spectrum lines which will be discussed in Section 3.2.

The slit width of 0.4 mm was found sufficient to give measurable intensity decay curves for wavelengths above 3000 Å. However in the region 1800-3000 Å, the slit width had to be increased to 1.0 mm for all except the strongest

lines.

The region from 1100-1800 Å was also investigated using a sodium salicylate coated window at the spectrometer exit slit. This coating fluoresced in the violet region of the spectrum and the fluorescent radiation should have been detected by the photomultiplier. In practice this arrangement proved too insensitive and no lines were seen below 1800 Å.

One final point can be made in connection with the optical arrangement. The optical alignment of the various components used in the 1968 set-up was greatly facilitated by the use of a small helium-neon laser kindly made available by the staff of the Radiation Research Laboratory.

2.5 The Photomultiplier

A photomultiplier is a high gain, low noise device which converts light power striking on the photosensitive cathode into electric current. The output current is propotional to the input light intensity. In order to determine which photomultiplier tube was most suitable for this experiment, the signal current to be expected was estimated as follows:

The ion beam current is about 0.5 μA, corresponding to 3×10^{12} ions crossing the target per second. As was mentioned in Section 2.2, the singly ionized molecules were used to bombard the target and dissociated into atoms after

emerging from the target, giving 6×10^{12} atoms/sec on the down stream side of the target. Assuming that the atoms are nearly all excited and the lifetime of a typical spectrum line is 5 nsec then for 1 MeV O_2^+ incident beam half of the excited states will decay within 1 cm. Since 0.2 mm of the beam was imaged to the slit of the spectrometer in the 1967 arrangement, the number of atoms radiating within 0.2 mm at 1 cm from the target, using Eq. (2.6), will be

$$\frac{\Delta N}{N_o} = e^{-\ell_1/v\tau}(1 - e^{-(\ell_2-\ell_1)/v\tau}) \simeq \frac{1}{100}$$

in this case, because $e^{-\ell_1/v\tau}$ was assumed to be 0.5.

The geometric factor of the instrument allowed only about 1/2000 of the photons emitted to reach the entrance slit of the spectrometer. Thus a typical line that has an intensity which comprises 1/500 of the total intensity would have a number of photons arriving at the photomultiplier cathode given by

$$6 \times 10^{12} \times \frac{1}{100} \times \frac{1}{2000} \times \frac{1}{500} \times \frac{1}{2} = 3 \times 10^4$$

photons/sec, where a factor of 1/2 has been introduced because, as will be seen in Section 3.2, the instrumental width of the line is about the same as the Doppler broadening, thus about half of the photons will be lost since the exit slit was set to the same width as that for the entrance slit. Let the quantum efficiency of the cathode of the photomultiplier used be 10%, and amplification be 10^7, then

the current expected is $3x10^{10}$ electrons/sec, or $5x10^{-9}$ A. With this low current level, an extremely high gain and low noise level photomultiplier must be used. The Model 6256S from EMI was reputed to show a dark current at room temperature of only $0.5x10^{-9}$ A for a gain of $4x10^{7}$ (with an overall voltage of 1750 volts). This appeared to be the best available and the 6256S was therefore chosen for these experiments.

The high dependence of the gain on supply voltage makes the regulation and stability of the power supply very critical. A variation of applied voltage by only 0.01% will cause a variation of the amplification by 1%. To test the stability of the power supply, the photomultiplier was exposed to a constant light source and a constant voltage was applied. No variation of the output current was obtained, proving the power supply to be satisfactory.

Since the signals to be expected are so low, further consideration was given to the problem of noise. The noise current of a photomultiplier has the following sources:

a) Thermionic emission from the cathode and dynodes.

b) Field emission from the cathode and dynodes.

c) Secondary emission due to the bombardment of the cathode or dynodes by positive ions.

d) Leakage current across the insulators

suporting the electrodes.

e) Back ground radiation of the laboratory.

g) Shot noise due to statistical fluctuations in the electron flow of the circuit.

Back ground radiation, such as γ-ray or neutron, could introduce some noise to the photomultiplier and can be reduced by surrounding the photomultiplier with lead shielding. Field emission noise was avoided by operating below the critical field strength. Thermionic emission from the cathode and dynodes is, however, the major source of dark current. Thermal noise is expected to obey the Richardson-Dushman equation:

$$J = AT^2 e^{\phi/kT} \qquad (2.7)$$

where $A = 120\ A\cdot deg^2/cm^2$,

T = Absolute temperature in °K,

k = Boltzman constant = 1.38×10^{-23} watt·sec/deg,

ϕ = Work function of the cathode material.

A glance at Eq. (2.7) would indicate the cooling of the photomultiplier would decrease the current markedly. It was found in practice that the dark current for the 6256S could be decreased by a factor of about 10 by cooling with dry ice, but the moisture condensed in the voltage divider make the amplification decrease by a factor of 10 or sometimes even

more. It was noted that the dark current was in the order of 100 nA when the high voltage was first applied and decreased to about 10 nA in 30 minutes. It was also found that the signal to noise ratio could be somewhat improved by operating the photomultiplier at voltages below those recommended by the manufacturer.

The signals found in practice were typically ten times that due to noise for the strongest lines. Lifetimes were recorded only for lines giving a signal to noise ratio of at least three.

CHAPTER III

ANALYSIS

3.1 Evaluation of Radiative Lifetimes from the Decay curves

Each raw decay curve consisted of the actual decay signal modified by an additive constant due to background radiation and noise. A smooth curve was drawn through the center of the raw data. The additive constant was then subtracted by switching the zero reading of the scale to a suitable level. This level was normally found by recording the signal from the ion beam before it struck the foil. It was found that the signal would decay back to this level if the radiation was scanned sufficiently far down stream of the foil. Data were then taken from the modified curve at intervals of one millimeter along the beam, as shown by the side-event marker operating from the indicator wheel shown in Fig. 2.4. The logarithm of the intensity was then plotted against distance along the beam. If the line was unblended and cascade-free, the curve on the semilogarithmic plot was a straight line having a slope equal to minus reciprocal of the mean lifetime of the upper level. For cases in which two or more lines were unresolved, or in which the upper level was repopulated by cascade transitions from higher levels the curve on the semilogarithmic plot was non-linear. The appearance of this curve for cases in which repopulation is due to cascade transitions may be understood as follows: For a cascade transition, Eq. (1.14) can be rewritten as

$$N_i = (N_{io} - \frac{A_{ki}N_{ko}}{\alpha_i - \alpha_k})e^{-\alpha_i t} + \frac{A_{ki}N_{ko}}{\alpha_i - \alpha_k}e^{-\alpha_k t} \qquad (3.1)$$

which can be written in the following form

$$I = Ae^{-t/\tau_i} + Be^{-t/\tau_k} \qquad (3.2)$$

where
$$A = kA_{ij}(N_{io} - \frac{A_{ki}N_{ko}}{1/\tau_i - 1/\tau_k}) \qquad (3.3)$$

$$B = kA_{ij}\frac{A_{ki}N_{ko}}{1/\tau_i - 1/\tau_k} \qquad (3.4)$$

since $I = kA_{ij}N_i$, k being the product of geometric factor times quantum efficiency of the instrument, and A_{ij} is the transition probability as defined before. From Eq. (3.3) and (3.4),

$$\frac{A}{B} = (1/\tau_i - 1/\tau_K)\frac{N_{io}}{A_{ki}N_{ko}} - 1 \qquad (3.5)$$

Therefore A and B may have opposite signs or both positive depending upon whether the first term on the right hand side of Eq. (3.5) is greater or less than 1. In the case where A and B are both positive, τ_i must be smaller than τ_k, thus both the lifetimes for k and i states are determined by observing the transition i→j.

For two unresolved cascade-free lines, the intensity equation is written as

$$I = Ae^{-t/\tau_1} + Be^{-t/\tau_2} \qquad (3.6)$$

Here both A and B must be positive. A semilogarithmic plot

of Eq. (3.6) will result in a curve for which the gradient flattens with time. This may also be seen by taking the second derivative of lnI with respect to t:

$$\frac{d^2 \ln I}{dt^2} = \frac{\left(1/\tau_1\right) A e^{-t/\tau_1} + \left(1/\tau_2\right) B e^{-t/\tau_2}\right)^2}{I^2} +$$

$$\frac{\left(1/\tau_1\right)^2 A e^{-t/\tau_1} + \left(1/\tau_2\right)^2 B e^{-t/\tau_2}}{I} \qquad (3.7)$$

which is, of course, greater than zero because both A and B are positive.

Considering only the two cases, a cascade repopulated single line and two unresolved cascade-free lines, the following types of decay curve are to be expected in the observations:

i) Type A linear, due to single cascade-free lines or one of the components in Eq. (3.5) or (3.6) is negligible.

ii) Type B concave upward, due to unresolved lines or cascading with A and B both positive.

iii) Type C concave downward, due only to cascade repopulated line with one of A or B negative.

Type A is trivial and has been shown in Fig. 1.1. Type B and C are given in Fig. 3.1.

In order to improve the accuracy and save the time needed in the analysis of the curved decay, a computer program was developed which computes the value of I for every

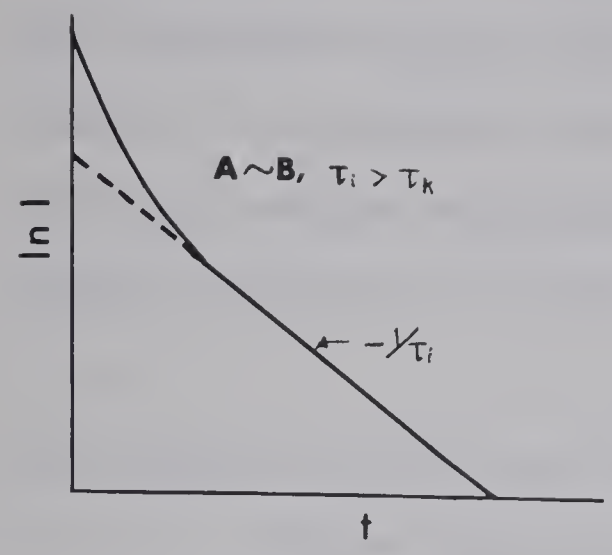

TYPE B

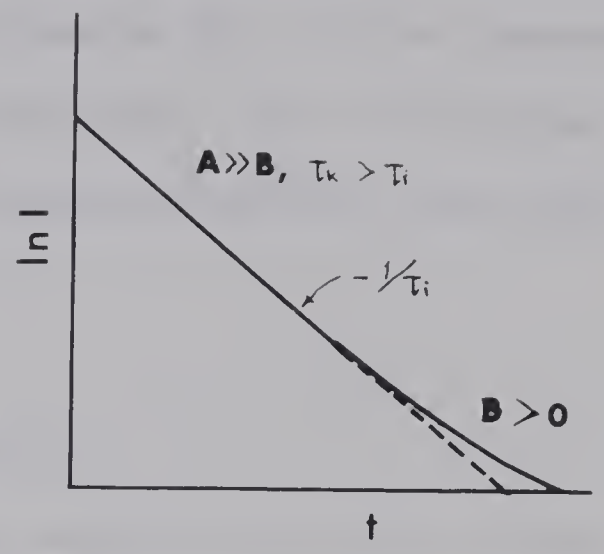

TYPE B

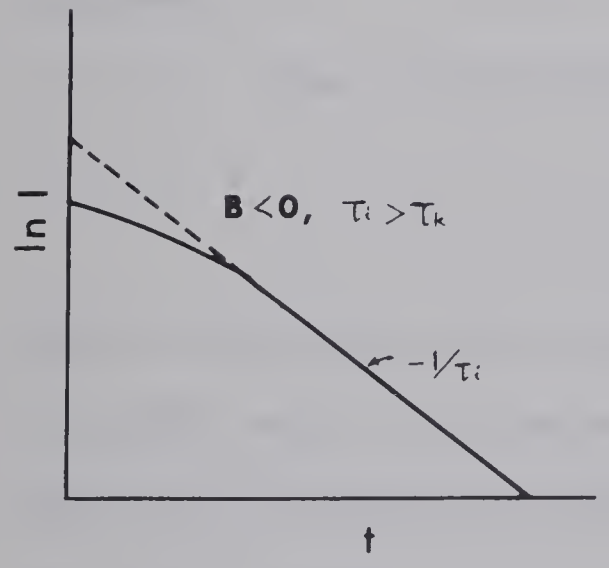

TYPE C

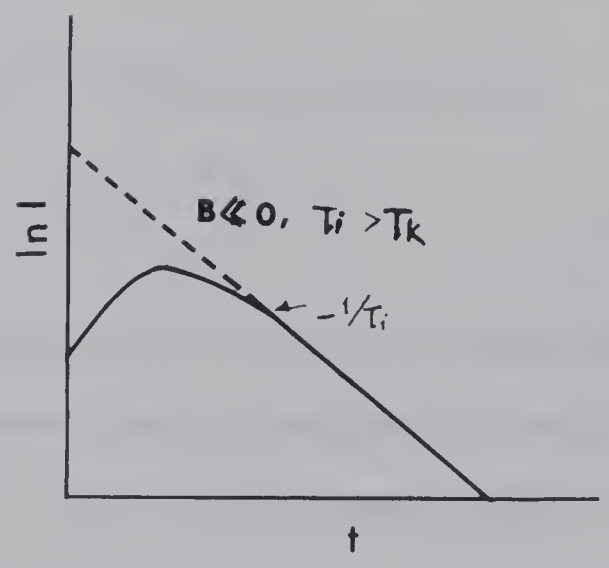

TYPE C

FIG. 3.1 Diagram of some possible decay types.

possible combination of A, B, τ_1 and τ_2, and then compares them all with the observed decay curve. The output gives the lifetimes having the least squares fit to the observed curve. Two programs were actually used, one for coarse fitting and the other one for accurate fitting using the result of coarse fitting.

3.2 Beam Velocity and Line Profile

Since the photons were emitted from high speed moving ions, Doppler effect wavelength shifts were seen, which could be used to measure directly the beam velocity. The reliability of this measurement was investigated as follows:

The relativistic Doppler effect is given by

$$\lambda_o - \lambda = \lambda_o(\beta\cos\theta + \frac{1}{2}\beta^2 + \cdots) \qquad (3.8)$$

where β is the ratio of the source velocity to the velocity of light and θ is the angle between the direction of motion and the direction of observation. For these experiments β was 0.8%, hence the term in β^2 may be neglected. The observations were made in 3 different directions. If the energy loss in passing through the foil could be neglected, the shifts would be

for beam A ($\theta = 90°$) $\Delta\lambda = \lambda_o(\beta\cos 90°) = 0$,

for beam B ($\theta = 30°$) $\Delta\lambda = \lambda_o(\beta\cos 30°) = 0.866\beta\lambda_o$,

for beam C ($\theta = 10°$) $\Delta\lambda = \lambda_o(\beta\cos 10°) = 0.985\beta\lambda_o$.

At 1 MeV, the velocity for O_2^+ ions is 2.46×10^8 cm/sec, therefore the shifts expected for the line at 4376 Å were 0 Å for beam A, 31.1 Å for beam B, and 35.4 Å for beam C. The observed values were about 4% lower, which indicated that an energy loss of about 8% was suffered while traversing the foil. This was consistent with the estimated energy loss by Fink et al. (Fi 68). The lifetimes listed in Chapter IV are based on the beam velocity obtained by measuring the Doppler shifts.

In order to measure the shifts as precisely as possible, a mercury spectrum was superimposed on the recorded spectra by placing a small mercury discharge lamp several meters from the target chamber and allowing its light to be scattered by the chamber window onto the spectrometer slit. The resulting spectra will be given in Chapter IV.

The angle of observation is an important factor in the wavelength shift. The effect of the uncertainty in the direction of observation on the wavelength shifts for the 3 beams was investigated as follow:

The directions of the reflecting mirrors were accurately set by the machine shop, hence the possible error came from the alignment of the focusing device. Allowing an error of ±1° in the alignment, the uncertainty in the beam direction was ±0.5° because of the reflection of the mirrors. The uncertainties in the directions for beam B and C then gave

$$\left(\frac{\Delta\lambda}{\lambda\beta}\right)_B = \cos\left(30 \pm \frac{1}{2}^\circ\right) = 0.866 \pm 0.004$$

and $$\left(\frac{\Delta\lambda}{\lambda\beta}\right)_C = \cos\left(10 \pm \frac{1}{2}^\circ\right) = 0.985 \pm 0.002$$

for beam B and C respectively. The uncertainty for beam A was not halved by reflection, hence

$$\left(\frac{\Delta\lambda}{\lambda\beta}\right)_A = \cos(90 \pm 1^\circ) = 0 \pm 0.0175$$

Hence for the wavelength shifts

$\left(\frac{\Delta\lambda}{\lambda\beta}\right)_B - \left(\frac{\Delta\lambda}{\lambda\beta}\right)_A = 0.866 \pm 0.018$, an uncertainty of 2.1%

$\left(\frac{\Delta\lambda}{\lambda\beta}\right)_C - \left(\frac{\Delta\lambda}{\lambda\beta}\right)_A = 0.985 \pm 0.018$, an uncertainty of 1.8%.

Thus this method was expected to give the velocity to an accuracy of about 2%.

Besides wavelength shifts, the Doppler effect gives rise to broadening of the spectral lines. Fig. 3.2 illustrates the cause of the broadening. Photons from a given point along the beam can enter the spectrometer for a range of angles with respect to the beam direction. The mirrors used in the focusing device were 5 cm in diameter. However, not all the mirror surface was used because the instrument aperture of the spectrometer was only f/6.8. This is illustrated in Fig. 3.3. The limiting wavelength, from Eq. (3.1) and neglecting the second order term in β, will be

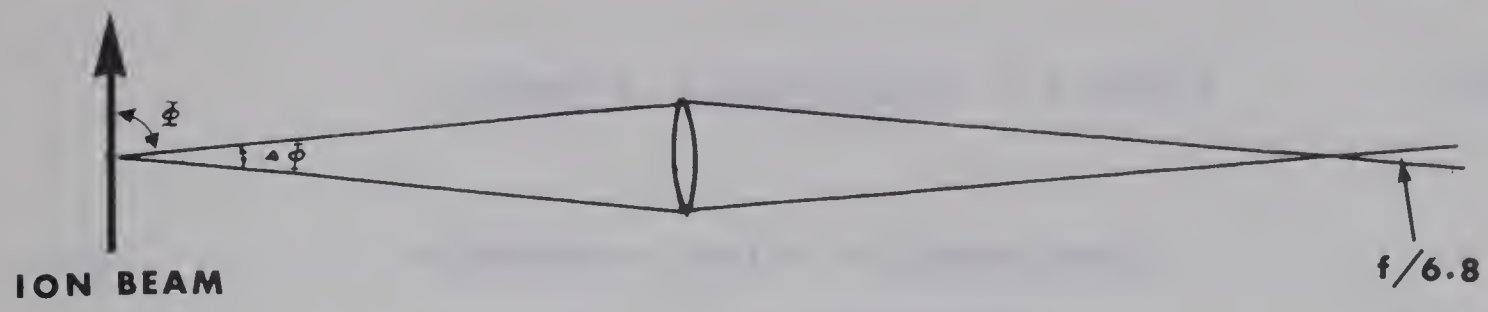

FIG. 3.2 Illustration of cause of line broadening.

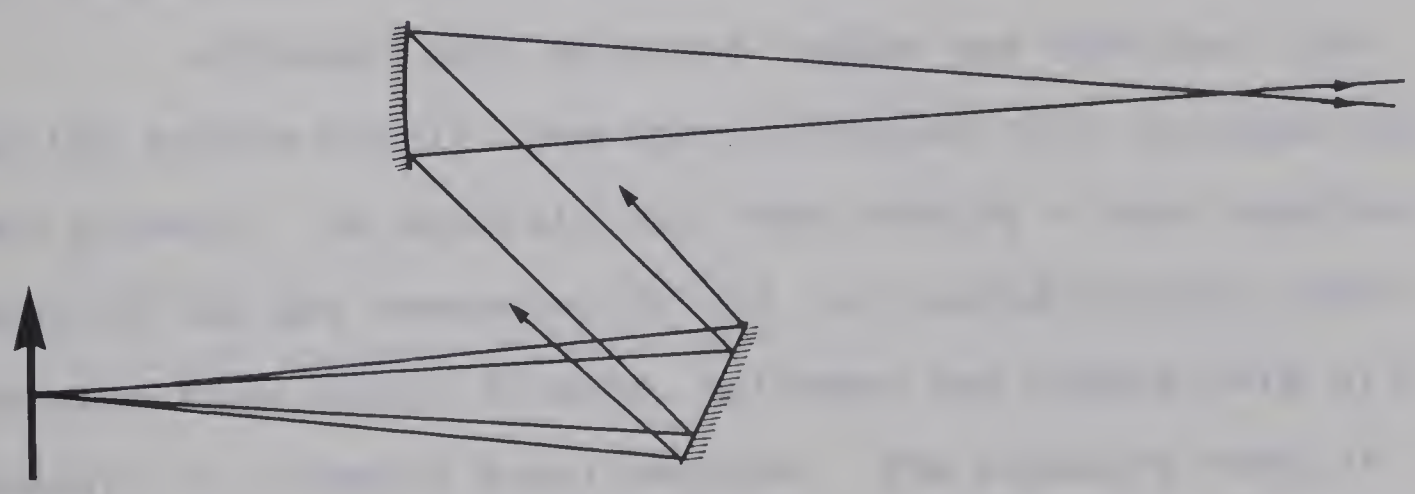

FIG. 3.3 Diagram showing that only centers of the mirrors were actually used.

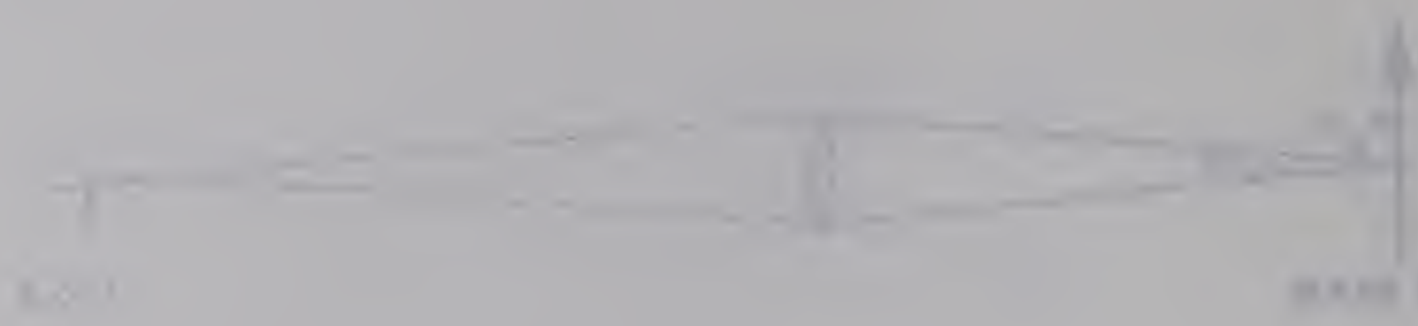

$$\lambda_o \beta \cos\phi = \lambda_o \beta \sin(\Delta\phi/2) \simeq \lambda_o \beta \Delta\phi/2 \qquad (3.9)$$

and
$$\lambda_o \beta \cos(\phi + \Delta\phi) = -\lambda_o \beta \sin(\Delta\phi/2)$$
$$\simeq -\lambda_o \beta \Delta\phi/2. \qquad (3.10)$$

Since $\Delta\phi$ is in general very small. Therefore the range of wavelength will be $\lambda_o \beta \Delta\phi$. In this experimental arrangement $\Delta\phi$ was about 0.15 radian and $\beta \simeq 0.8\%$ for 1 MeV O_2^+ incident beam, therefore at 4000 Å the broadening was about 5 Å. Fig. 3.4 gives the comparison between unbroadened mercury line and broadened oxygen line having the same instrumental width.

3.3 Impurities in the Source

Although only purified oxygen was admitted into the ion source bottle, the spectra showed that nitrogen was also present. An analysis was then made by a mass spectrometer of the gas remaining in the ion source bottle, which revealed that carbon dioxide, nitrogen and oxygen were all present in roughly equal amounts. The pressure tank of the accelerator was filled with carbon dioxide and nitrogen at high pressure in order to provide insulation at the high voltage terminal. An inwards leakage of the source bottle under the high pressure is the most likely cause of the impurities. Since the resolution of the analyzing magnet

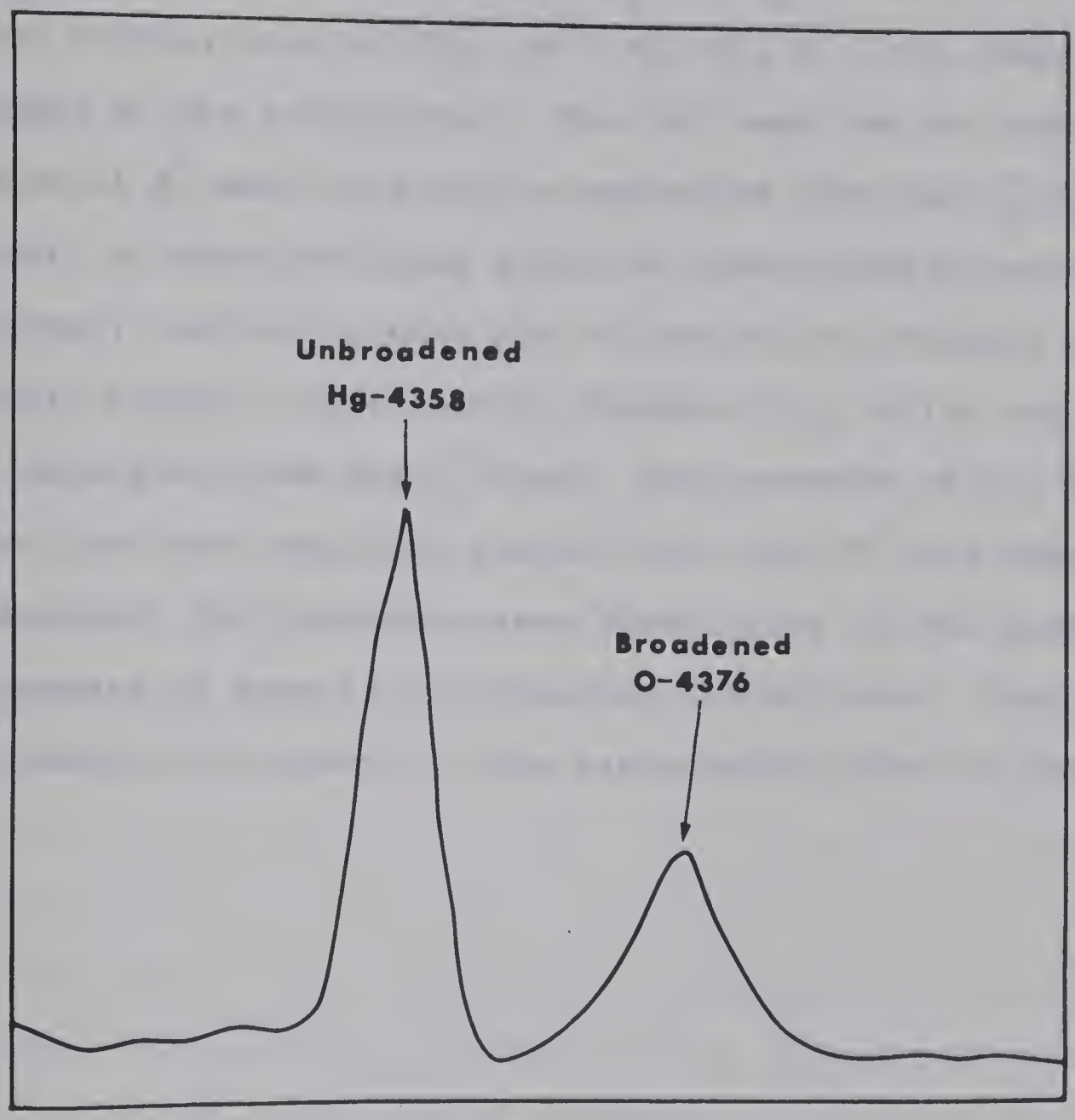

FIG. 3.4 A comparison between broadened and unbroadened line profiles.

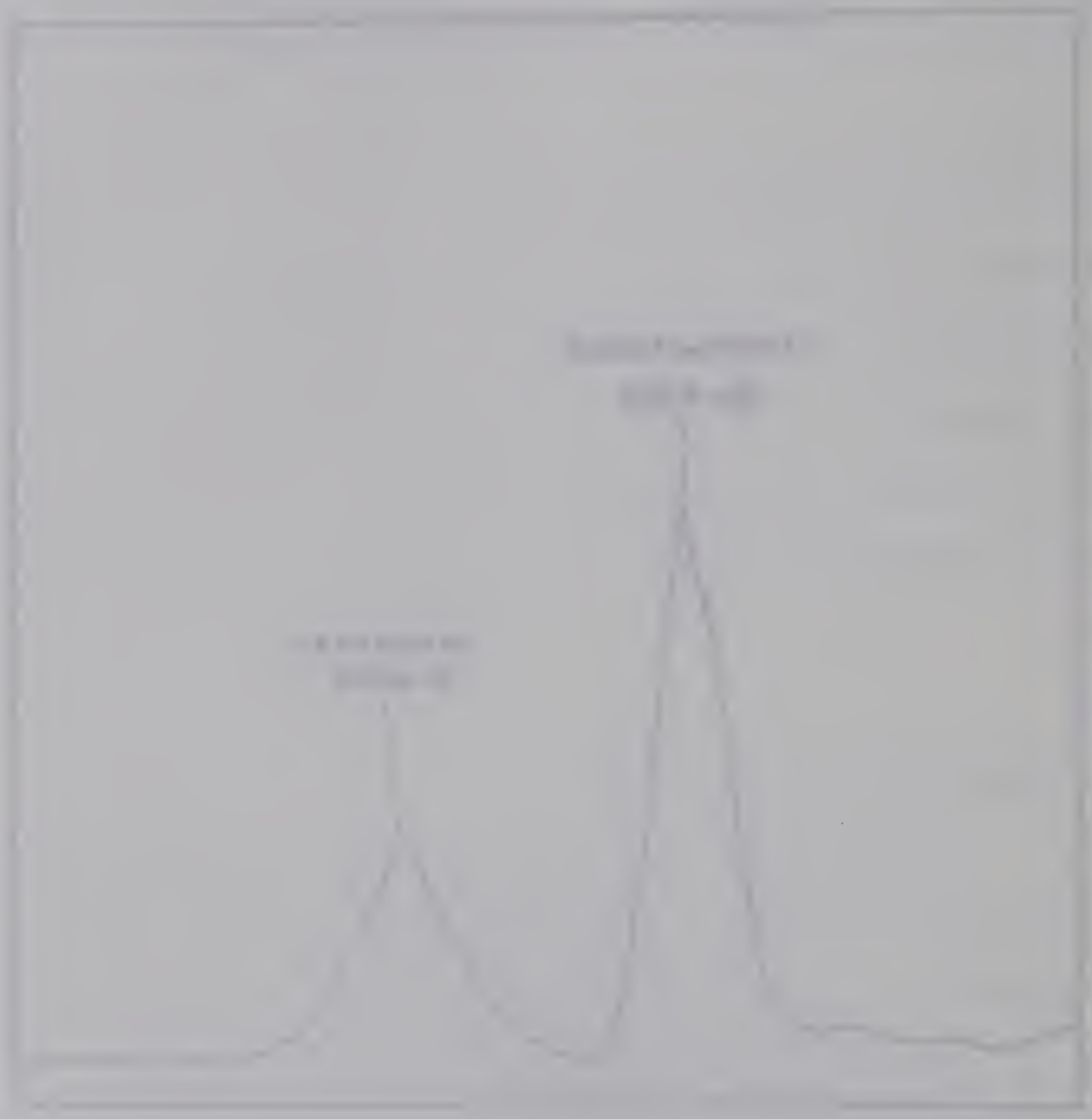

was not enough to separate the N_2^+ from the O_2^+, data were therefore also obtained for nitrogen lifetimes in addition to those for oxygen. With CO_2, N_2 and O_2 present in the source bottle, ions of CO_2^+, CO^+, N_2^+, O_2^+, C^+, etc. were produced by the accelerator. The CO^+ beam had the same mass as that of N_2^+ and could not be separated from the O_2^+-N_2^+ beam. However, no spectrum lines could be unambiguously assigned to carbon, indicating that the rf ion source produced predominantly singly ionized carbon dioxide, CO_2^+, which was very well separated from the O_2^+ beam. The presence of CO_2 in the source, and the resulting possibility that CO^+ had been accelerated, did introduce some uncertainty in the spectrum assignments of some of the observed transitions. This has been taken into account in the assignments given in Chapter IV.

CHAPTER IV

RESULTS

4.1 The Spectrum

The spectra produced by the O_2^+-N_2^+ beam were recorded in the range 1800-5500 Å both at 1 MeV and 1.5 MeV, and in the range 2000-2600 Å at 0.5 MeV. Significant variations in the appearance of the spectrum with change in beam energy were noted, as had previously been recorded by other workers (Fi 68, Le 67).

The wavelengths of the spectrum lines were determined by using the wavelength marker of the spectrometer which gave a signal pulse every 5 Å. This signal was fed to the side-event marker on the chart recorder. The wavelength assigned to a line was the average of those obtained from the spectra at 1 MeV and 1.5 MeV. The uncertainty were ±1 Å in most cases, and ±2 Å for very weak and very strong lines (several very strong lines in the spectra were off scale, therefore the wavelength determinations were less accurate).

In the assignments of observed lines, the published tables by Moore (Mo 50, Mo 59) have mainly been used to identify the transitions, assuming that only oxygen and nitrogen lines were present in the spectra. The report by Bashkin et al. (Ba 66) has also been used to assist in distinguishing between the various possible assignments. This report was useful because it classified the lifetimes qualitatively as being very short, short, medium or long so

that a comparison with the results of this experiment could be made. The work of Fink et al. (Fi 68) and of Lewis et al. (Le 67) with nitrogen was also helpful.

4.1 Beam Velocity

Fig. 4.1 presents the wavelength shifts obtained in the beam velocity measurements. Four runs of the measurements were actually taken, resulting in a value of $(2.36 \pm 0.01) \times 10^8$ cm/sec. The line chosen for the observation was of oxygen at 4376 Å, hence the velocity of the N_2^+ ions would be 7% higher than that of the O_2^+ ions. It may also be noted that a relatively faint peak at about 4345-4351 Å was also shifted to the violet on the 30° and 10° tracings. The bars on the right side of each tracings represent noise levels.

4.3 Lifetimes

In the 1967 observations about 100 lifetimes were obtained. Instead of taking the actual spectrum and determining the wavelengths independently, the listed wavelengths in Bashkin et al.'s report (Ba 66) were taken and the spectrometer was set to these wavelengths in turn. The decay curve for each spectrum line was then obtained by scanning the focusing device along the beam. The accuracy of the time scale depended entirely on the uniformity of the scanning speed and of the recorder paper speed, as well as the accuracy of the estimation of the beam speed. Using a

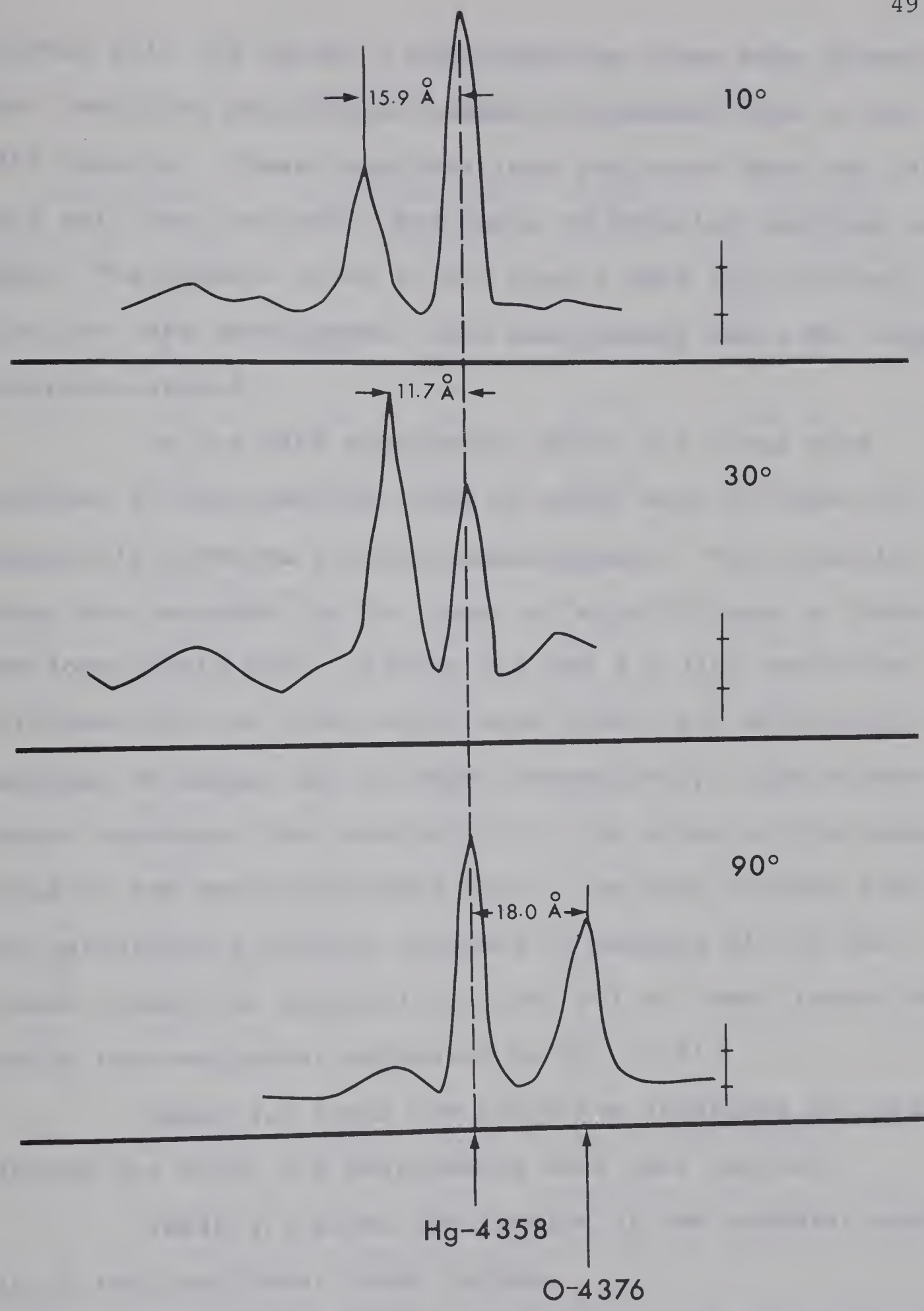

FIG. 4.1 Tracings of Doppler shifted oxygen lines.

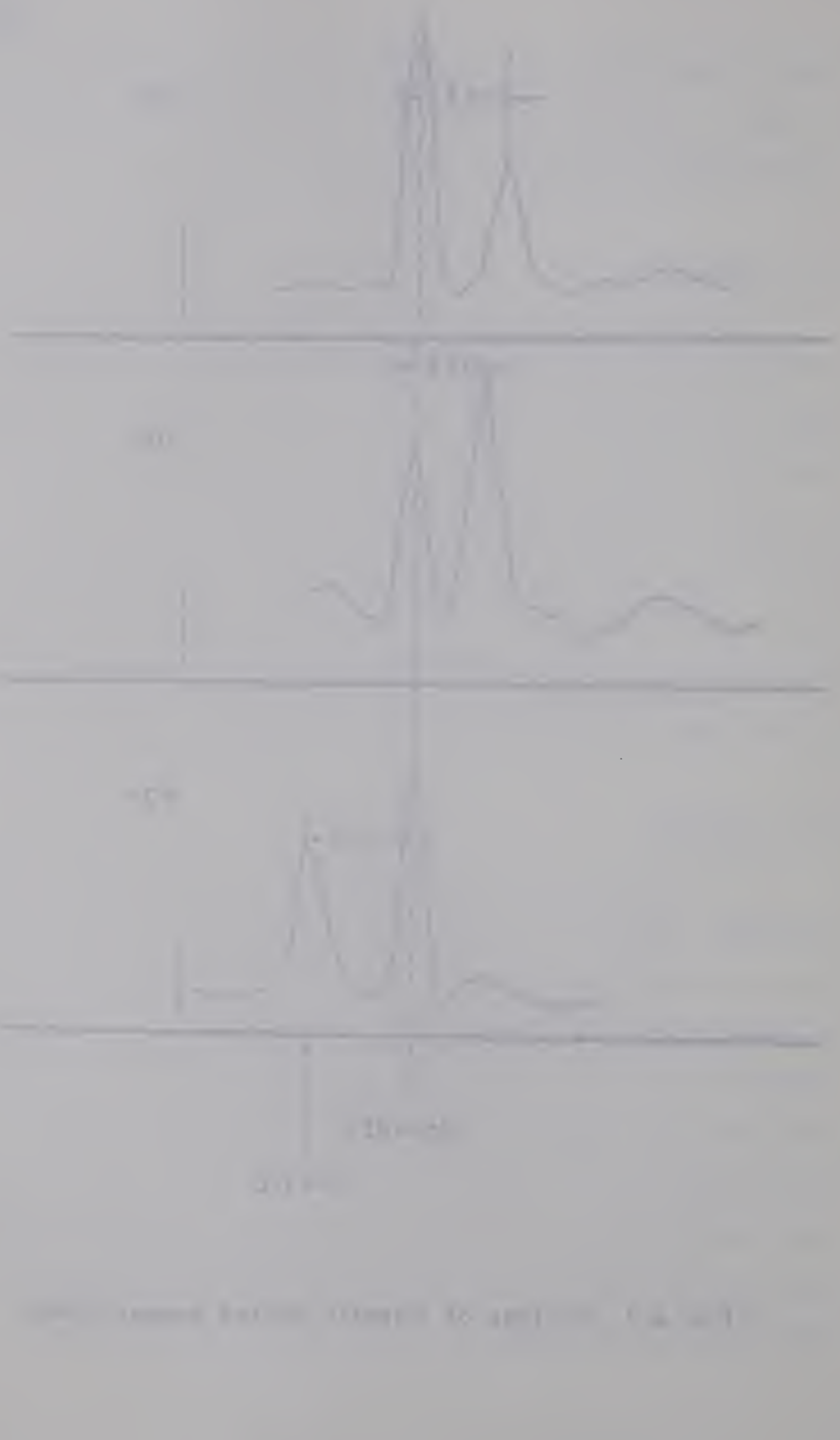

thicker foil (25 $\mu g/cm^2$), more spectrum lines were present, thus resulting in a higher number of blended lines in the 1967 results. These considerations indicated that the 1967 data were less reliable, and hence no detailed analysis was made. The results given in the thesis were all obtained with the 1968 arrangement. The beam energy was 1 MeV unless otherwise stated.

In the 1968 experiments about 100 lines were obtained in the spectrum, some of which were too weak for reasonably accurate lifetime measurements. The intensity decay was recorded for 64 lines, of which 35 gave a linear semilogarithmic plot. Tables 4.1 and 4.2 list radiative lifetimes for the lines which were linear and definitely assigned to oxygen and nitrogen respectively. The errors quoted represent the uncertainty in the slope of the straight lines on the semilogarithmic plot. The last columns give the calculated lifetimes obtained by summing all of the listed transition probabilities (Wi 66) to lower levels and taking the reciprocal according to Eq. (1.5).

Table 4.3 lists the radiative lifetimes for transitions for which the assignments were less certain.

Table 4.4 gives the results of the computer analysis of the non-linear decay curves.

Table 4.5 compares lifetimes which were obtained in the experiment with those measured by other workers (Le 67, Ba 68, De 68, Fi 68).

TABLE 4.1

RADIATIVE LIFETIMES FOR OXYGEN

Wavelength Observed (±2 Å)	Wavelength Listed (NBS[a,b])	Ion	Multiplet Number	Upper Level	Lifetime Observed (nsec)	Lifetime Calculated (nsec)
2296	2293.32 2300.35	OII[c]	19[a]	$3p'\ ^2P°$	8.6±0.4	7.1
2981	2983.78	OIII	18[a]	$3p\ ^1D$	4.6±0.2	4.5
3452	3450.94 3455.12	OIII	25[b]	$3d\ ^5F$	6.4±0.3	6.0
4073	4072.164 4075.868	OII	10[b]	$3d\ ^4F$	6.7±0.1	5.1
4123	4123.90	OV	4[b]	$3p\ ^3D$	5.3±0.1	20.5
4144	4143.77 4146.09	OII	106[b]	$sp^3 3d^6D°$	4.6±0.3	47.6
4155	4156.54 4158.76	OII OV	19[b] 11[b]	$3d\ ^4P$ $3d\ ^3P°$	4.9±0.2	0.25 8.7
4254	4253.74 4253.98	OII	101[b]	$4f'\ ^2H°$	6.9±0.2	3.8
4345 4350	4345.552 4349.426	OII	2[b]	$3p\ ^4P°$	6.2±0.2	9.7
4592	4590.971	OII	15[b]	$3p'\ ^2F°$	8.7±0.3	9.0

a. C. E. Moore, N.B.S. Circular 488 (1950)

b. C. E. Moore, N.B.S. Technical Note 36 (1959)

c. This line may possibly be 2296.89 Å for CIII, in which case τ would be 8.1±0.4 nsec compared with a theoretical value of 2.8 nsec.

TABLE 4.2

RADIATIVE LIFETIMES FOR NITROGEN

Wavelength		Ion	Multiplet Number	Upper Level	Lifetime	
Observed (±2 Å)	Listed (NBS[a,b])				Observed (nsec)	Calculated (nsec)
1907	1908.11	NIII	27[a]	$4f\,^2F$	2.2±0.1	0.91
1922	1920.86 1921.46	NIII	29[a]	$4f\,^4D$	2.2±0.1	0.97
2065	2063.50 2063.99	NIII	30[a]	$4f\,^2G$	2.4±0.1	0.88
2247	2247.92 2248.88	NIII	23[a]	$4p\,^2P°$	3.1±0.3	6.1
2861	2862.26	NIII	26[a]	$6g\,^2G$	5.8±0.5	---
3353	3353.78 3354.29	NIII	5[b]	$3p\,^4P$	5.8±0.3	5.7
3366	3367.36	NIII	5[b]	$3p\,^4P$	5.4±0.3	5.7
3437	3437.162	NII	13[b]	$3p\,^1S$	5.3±0.3	4.2
3481	3478.69 3482.98 3484.90	NIV	1[b]	$3p\,^3P°$	7.3±0.5	8.6
3940	3938.52	NIII	8[b]	$3d\,^2D°$	3.0±0.1	10.4
3995	3994.996	NII	12[b]	$3p\,^1D$	6.1±0.3	6.3
4199	4195.70 4200.02	NIII	6[b]	$3p\,^2D$	2.3±0.1	10.0
4241	4241.787	NII	47[b] 48[b]	$4f\,^1F$ $4f\,^3F$	5.9±0.3	4.6 4.7
4289	4288.21 4288.72 4290.55	NIII	unclassified[b]		4.6±0.3	---

a. C. E. Moore, N.B.S. Circular 488 (1950)
b. C. E. Moore, N.B.S. Technical Note 36 (1959)

TABLE 4.3

RADIATIVE LIFETIMES FOR UNASSIGNED TRANSITIONS

Wavelength (±2 Å)	Lifetime (nsec)		Possible Assignment	
	Oxygen	Nitrogen	Ion	Multiplet
2147	3.9±0.2	3.6±0.2	-	-
2510[c]	2.7±0.1	2.5±0.1	-	-
2831	5.6±0.3	5.2±0.3	-	-
2883	5.9±0.7	5.4±0.7	OI	10[a]
3063	1.98±0.05	1.88±0.05	OIV	1[b]
3794	3.14±0.08	3.03±0.08	OIII	2[b]
3839	3.35±0.06	3.24±0.06	NII	30[b]
4041	6.2±0.1	5.8±0.1	-	-
4267[c]	5.5±0.1	5.1±0.1	-	-
4656[c]	5.1±0.1	4.7±0.1	OI	18[b]
			OII	1[b]
5027[c]	3.9±0.1	3.6±0.1	NII	19,64[b]

a. C. E. Moore, N.B.S. Circular 488 (1950)

b. C. E. Moore, N.B.S. Technical Note 36 (1959)

c. Possibly due to transitions in carbon, in which case the lifetime given in the column labelled "Nitrogen" would apply.

TABLE 4.4

RESULTS OF COMPUTER LEAST-SQUARES FIT TO

$A \exp(-t/\tau_1) + B \exp(-t/\tau_2)$

Wavelength (±2Å)	Ion	A	τ_1(nsec)	B	τ_2(nsec)	Mean Square Deviation
1847	----	14.0	2.0	7.4	5.0	0.06
1884	NIII	40.2	1.9	10.6	7.8	0.09
1884[a]	NIII	29.8	2.3	14.6	2.5	0.55
2014	----	34.6	3.0	- 7.2	11.3	0.17
2147	----	14.4	2.1	7.0	0.8	0.02
2247[b]	NIII	26.4	3.7	- 6.4	9.8	0.05
2247[d]	NIII	38.6	3.7	- 3.6	8.1	0.20
2247[a]	NIII	31.8	3.1	10.6	1.9	0.10
2318	NII	16.0	4.6	3.8	3.5	0.06
2430	OII	30.0	4.0	- 8.4	9.6	0.11
2450[b]	OII,OIII	25.8	4.0	- 2.0	5.7	0.10
2450	OII,OIII	21.8	2.1	5.4	9.6	0.13
2645	NIV	22.0	2.1	18.2	7.4	0.17
2645[a]	NIV	37.2	1.8	27.0	6.4	0.07
2727	(OII)	25.4	4.5	- 3.6	0.9	0.03
2819	(NII)	25.2	4.6	- 1.0	5.7	0.14
2981[d]	OIII	29.4	4.7	1.8	3.6	0.07
3047	OIII	23.2	3.6	2.6	4.3	0.16
3329[c]	NII,OIII	20.6	5.5	13.4	1.8	1.93
3366[b,d]	NIII	39.6	4.1	- 3.6	0.6	1.22
3366[d]	NIII	29.2	5.3	11.8	5.4	0.04

Wavelength (±2Å)	Ion	A	τ_1 (nsec)	B	τ_2 (nsec)	Mean Square Deviarion
3385	OIII,OIV	16.8	12.1	7.4	1.8	0.10
3437[d]	NII	24.0	5.1	- 1.6	0.9	0.03
3452[d]	OIII	22.4	7.0	15.8	6.7	0.18
3703[c]	OIII, CIII	26.2	7.2	-15.2	1.4	0.14
3772[c]	OIII, NIII	44.2	6.0	-31.2	1.3	1.93
3919	NII,CII	9.4	2.0	8.6	4.6	0.01
4000	NIII,NII	29.8	2.8	8.2	8.8	0.10
4090	OII	56.6	5.2	- 8.2	1.1	0.38
4099[b,c]	NIII,OII	66.2	6.7	- 4.4	1.3	0.55
4099[c,d]	NIII,OII	39.8	5.5	- 0.8	4.3	0.08
4134[c]	NII,OIII	26.4	5.5	- 2.8	7.2	0.07
4155[d]	OII	23.0	4.7	- 6.4	5.0	0.02
4241[d]	NII	44.8	6.0	- 1.4	1.2	0.11
4378[c]	OII,NIII	43.0	8.2	11.8	1.8	0.18
4514	NIII, CIII	57.6	19.3	-23.2	4.8	0.51
4533	NIII	19.8	6.0	22.6	13.7	0.08
4647[c]	OII,CIII	38.6	8.0	- 8.0	1.8	0.07
4863[c]	NIII, (OII)	65.4	18.0	- 8.6	2.6	0.07
5002	NII	72.6	10.2	-16.8	2.4	0.15
5176[c]	NII, (OII)	45.0	3.1	- 4.8	2.8	0.11
5532	NII	29.0	25.7	5.0	5.6	0.04

a. The measurement was made at 1.5 MeV beam energy.
b. The measurement was made at 0.5 MeV beam energy.
c. The lifetimes given are for oxygen, those for carbon or nitrogen should be reduced by 7%.
d. The results show that this line should be classified as giving a linear plot.

TABLE 4.5

COMPARISON WITH DATA OBTAINED BY OTHER WORKERS

Wavelength (±2Å)	Ion	τ(nsec) Observed	τ(nsec) Denis et al.[a]	τ(nsec) Lewis et al.[b]	τ(nsec) Bashkin et al.[c]	τ(nsec) Fink et al.[d]
2247	NIII	3.1±0.3	2.6	1.24	---	---
3353	NIII	5.8±0.3	5.2	5.71	---	---
3366	NIII	5.4±0.3	5.2	5.84	---	---
3437	NII	5.3±0.3	4.1	---	---	---
3481	NIV	7.3±0.5	8.2	9.7	---	8.7
3940	NIII	3.0±0.1	4.3	---	---	3.0
3995	NII	6.1±0.3	7.0	---	---	---
4073	OII	6.7±0.1	---	---	10.8	---
4199	NIII	2.2±0.1	2.1	1.7	---	---
4254	OII	6.9±0.2	---	---	7.0±0.6	---
4289	NIII	4.6±0.3	---	4.2	---	---
4345	OII	6.2±0.2	---	---	5.7	---

N. B. All data are for 1 MeV incident energy.

a. A. Denis et al., C. R. Acad. Sc. Paris 266 (1968) 64

b. M. R. Lewis et al., Phys. Rev. 164 (1967) 94

c. S. Bashkin, private communication (1968)

d. U. Fink et al., J. Opt. Soc. Am. 58 (1968) 475

CHAPTER V

SUMMARY

The beam-foil technique has been employed to measure the radiative lifetimes for transitions due to oxygen and nitrogen ions. The observations were mainly made at a beam energy of 1.0 MeV and with foils of thickness of 10 $\mu g/cm^2$. About 100 spectral lines were detected in the range 1800 to 5500 Å. The decay curves of the 64 more intense lines were recorded. Of the 35 lines giving a single exponential decay, 10 lines were assigned to transitions in OII through OV, and 14 lines to transitions in NII through NIV. The lifetimes obtained range from 2 to 9 nsec. From the conparison with other workers given in Table 4.5 it may be concluded that the accuracy of the present measurements is about ±10%. A computer program has been developed to analyze the non-linear decay curves, with the intention to obtain the lifetimes for the cascade repopulated levels.

It is interesting to note that, although beam-foil spectroscopy has only been developed within the last five years, already one international conference has been devoted to the subject, the Beam-Foil Spectroscopy Conference held at the University of Arizona in November, 1967. At the International Symposium on the Physics of One- and Two-Electrons Atoms (Munich, September, 1968), a session on beam-foil spectroscopy was included and some of the results

contained in this thesis were presented. At least 40 papers have already been published on the subject. Three different observational techniques are being used. They are the photographic, direct-current and pulse-counting techniques. Lifetime data have been reported for ions of H, He^{+}, Li, Li^{+}, N^{+}- N^{4+}, O^{+}- O^{4+}, and Ne^{++}- Ne^{6+}. Elements of particular astrophysical interest are Si, Mg, Ca and Fe. Further advances in beam-foil spectroscopy will thus depend on the development of ion sources for these heavier elements. Bashkin et al. have used a standard rf ion source with argon gas and an iron (or aluminum) extraction canal to produce iron (or aluminum) ions (Ba 67). The metal ions are ejected by the collision of argon gas with the walls of the extraction canal. A beam current of 10^{-8} A was obtained. The Dufay group in Lyons has succeeded in producing beams of Li and Li^{+} by evaporation from a tungsten filament coated with lithium-aluminum silicate (Bu 67). It may also be possible to use large molecules containing atoms of interest (eg. SiF_4) as the source gas, but assignment of the transitions observed would be difficult because lines due to more than one element would appear.

The object of further study here will be to investigate more fully these various possibilities for heavy-ion sources, plus any other methods which may be developed. In addition, much useful work can still be done using elements contained in small gaseous molecules, i.e.

H, He, N, O, C (from CO_2), Ne, Ar, Kr, Xe, I, Cl, F, by extending the range of observation to shorter wavelengths. To this end it is planned to investigate more fully the various possibilities available for photon detection below 1800 Å, and thus to extend the observations at least down to 1100 Å.

REFERENCES

Ba 64 S. Bashkin, L. Heroux, and J. Show, Phys. Letters 13 (1964) 229

Ba 65 S. Bashkin, Science 148 (1965) 1047

Ba 66a S. Bashkin, D. Fink, P. R. Malmberg, A. B. Meinel and S. G. Tilford, J. Opt. Soc. Am. 56 (1966) 1064

Ba 66b S. Bashkin, R. K. Wangsness and L. Heroux, Phys. Rev. 151 (1966) 87

Ba 67 S. Bashkin, W. S. Bickel, H. D. Dieselman and J. B. Schroeder, J. Opt. Soc. Am. 57 (1967) 1395

Ba 68 S. Bashkin, private communication (1968)

Bi 66 W. S. Bickel and A. S. Goodman, Phys. Rev. 148 (1966) 1

Bi 67a W. S. Bickel. Appl. Opt. 6 (1967) 1309

Bi 67b W. S. Bickel and S. Bashkin, Phys. Rev. 162 (1967) 12

Bi 68 W. S. Bickel, J. Opt. Soc. Am. 58 (1968) 213

Br 62 L. Brewer, Rev. Sci. Insts. 33 (1962) 1450

Br 63 L. Brewer, R. A. Berg and G. M. Rosenblatt, J. Chem. Phys. 38 (1963) 1381

Bu 67 J-P. Buchet, A. Denis, J. Desesquelles and M. Dufay, C. R. Acad. Sc. Paris 265 (1967) 471

De 68 A. Denis, J. Desesquelles, M. Dufay and M-C. poulizac, C. R. Acad. Sc. Paris 226 (1968) 64

Di 52 R. W. Dichburn, Light (Blackie & Son, London,1963) 601

Fo 64 E. W. Foster, Reports on Progress in Physics 27 (1964) 469

Fi 68 U. Fink, G. N. McIntire and S. Bashkin, J. Opt. Soc. Am. 58 (1968) 475

Ka 63 L. Kay, Phys. Letters 5 (1963) 36

Ka 67 K. Karstensen and J. Schramm, J. Opt. Soc. Am. 57 (1967) 654

Kl 66 J. Z. Klose, Phys. Rev. 141 (1966)181

Le 67 M. R. Lewis, T. Marshall, E. H. Carnevale, F. S. Zimnoch and G. W. Wares, Phys. Rev. 164 (1967) 94

Ma 29 L. R. Maxwell, Phys. Rev. 34 (1929) 199

Ma 31 L. R. Maxwell, Phys. Rev. 38 (1931) 1664

Mo 50 C. E. Moore, An Ultraviolet Multiplet Table, NBS Circular 488 (1950)

Mo 59 C. E. Moore, A Multiplet Table of Astrophysical Interest, NBS Technical Note 36 (1959)

Ni 68 L. L. Nichols and W.E. Wilson, Appl. Opt. 7 (1968) 167

We 24 W. Wein, Ann. Physik 73 (1924) 32

Wi 66 W. L. Wiese, M. W. Smith and B. M. Glennon, Atomic Transition Probabilities, NSRDS-NBS 4-1 (1966)